SEDIMENTOLOGY the journal of the International Association of Sedimentologists

Sedimentology (2010) doi: 10.1111/j.1365-3091.2010.01179.x

The record of tidal cycles in mixed silici–bioclastic deposits: examples from small Plio–Pleistocene peripheral basins of the microtidal Central Mediterranean Sea

SERGIO G. LONGHITANO

Department of Geological Sciences, University of Basilicata, Campus Universitario di Macchia Romana, Viale dell'Ateneo Lucano 10, 95100 Potenza, Italy (E-mail: sergio.longhitano@unibas.it)

Associate Editor – Dave Mallinson

ABSTRACT

The Pliocene–Pleistocene peripheral marine basins of the Mediterranean Sea in southern Italy, from Basilicata and western Calabria to northern and eastern Sicily, represent tectonically formed coastal embayments and narrow straits. Here, units of cross-stratified, mixed silici–bioclastic sand, 25 to 80 m thick, record strong tidal currents. The Central Mediterranean Sea has had a microtidal range of *ca* 35 cm, and the local amplification of the tidal wave is attributed to tides enhanced in some of the bays and to the out-of-phase reversal of the tidal prism in narrow straits linking the Tyrrhenian and Ionian basins. The siliciclastic sediment was generated by local bedrock erosion, whereas the bioclastic sediment was derived from the contemporaneous, foramol-type cool-water carbonate factories. The cross-strata sets represent small to medium-sized (10 to 60 cm thick) two-dimensional dunes with mainly unidirectional foreset dip directions. These tidalites differ from the classical tidal rhythmites deposited in mud-bearing siliciclastic environments. Firstly, the foreset strata lack mud drapes and, instead, show segregation of siliciclastic and bioclastic sand into alternating strata. Secondly, the thickness variation of the successive silici–bioclastic strata couplets, measured over accretion intervals of 2 to 3 m and analysed statistically, reveal only the shortest-term, diurnal and semi-diurnal tidal cycles. Thirdly, the record of diurnal and semi-diurnal tidal cycles is included within the pattern of neap-spring cycles. Differences between these sediments and classical tidal rhythmites are attributed to the specific palaeogeographic setting of a microtidal sea, with the tidal currents locally enhanced in peripheral basins. It is suggested that this particular facies of mud-free, silici–bioclastic arenite rhythmites in the stratigraphic record might indicate a specific type of depositional sub-tidal environment of straits and embayments and the shortest-term tidal cycles.

Keywords Cyclicity, environment, microtidal, Pliocene–Pleistocene, silici–biocalcarenites, southern Italy, tidal, tidalites.

INTRODUCTION

Modern and ancient tidal deposits have been studied extensively (Flemming & Bartholomä, 1995; Alexander *et al.*, 1998), primarily because tidalites bear the important stratigraphic signatures of global tidal phenomena (Klein, 1971, 1998) and also because many tidal sandstone successions are major petroleum reservoirs (Messina *et al.*, 2009). Tidalites tend to bear the record of short-term astronomical periodicity on a daily, and monthly to annual, scale which is arguably the shortest-term geological cyclicity recognizable in the stratigraphic record (Alexander *et al.*, 1998). Common sedimentary features developed in a wide range of tidally dominated systems are known as tidal 'rhythmites' (Archer, 1995; Greb & Archer, 1995) which are deposits characterized by a rhythmical stacking of alternating sand and mud lamina couplets with systematic thickness changes (Reineck & Singh, 1975; Kvale *et al.*, 1989; Kvale & Archer, 1990; Archer, 1991, 1996; Dalrymple *et al.*, 1991; Dalrymple, 1992). The term 'rhythmites' was designed to define vertically accreted tidal facies, that commonly originate in intertidal to sub-tidal environments from oscillating flood and ebb tidal currents, and consequently related sandy/muddy deposition (Roep, 1991; Williams, 1991; Chan *et al.*, 1994; Choi & Park, 2000; Kvale, 2003; Mazumder & Arima, 2005; Greb & Archer, 2007). In recent times, this term has also been used to refer to laterally accreted deposits (foreset laminae or 'tidal bundles', see discussion in Coughenour *et al.*, 2009), if they are characterized by laminated to thinly bedded medium-grained to fine-grained sandstone, siltstone and mudstone of tidal origin that exhibit rhythmic change in lamina/bed thickness and grain size (Chan *et al.*, 1994). Although vertically accreted laminae and sandy bedform foresets are deposited via different mechanisms, the underlying energy forcing these processes is provided by tidal periodicities. Consequently, the term rhythmite can be applied consistently to these two different tidal facies (Allen & Homewood, 1984; Tessier & Gigot, 1989; Coughenour *et al.*, 2009). Time-series analyses of the couplet thickness variation have shown direct correlation with tidal cycles and can be a useful indicator of tidal harmonics, tidal-pattern dynamics and the astronomical forcing factors involved (Klein, 1998).

Tidalites vary from mud-rich to sandy and show a wide compositional range together with variable combinations of depositional structures, from thin heterolithic bedding (lenticular, wavy or mud-flasered) to 'bundled' cross-stratification and to bi-directional ('herringbone') or uni-directional cross-strata sets (see reviews by Klein, 1998 and, most recently, by Coughenour *et al.*, 2009). Many tidal systems are dominated by sediment of bioclastic or 'hybrid', mixed silici–bioclastic composition (Zuffa, 1980), derived from terrigenous and biogenic carbonate sources (Mount, 1984; Kamp *et al.*, 1988; Budd & Harris, 1990; Sieverding & Harris, 1991; Ginsburg & Cunningham, 1996; Warzeski *et al.*, 1996; Anastas *et al.*, 1997; Dorsey & Kidwell, 1999; Guertin *et al.*, 2000; Sanders & Höfling, 2000; D'Alessandro *et al.*, 2004; Wright *et al.*, 2005; Thrana & Talbot, 2006; Lubeseder *et al.*, 2009). The susceptibility of calcareous bioclastic material to hydraulic forces differs from that of siliciclastic material (Prager *et al.*, 1996), which may affect transport rates, cause differential sediment entrainment and lead to the formation of specific stratification varieties in mixed silici–bioclastic deposits (Meyer & Krauser, 1998).

The composition, grain-size range and depositional architecture of tidal deposits depend upon several factors: (i) the presence or absence of local carbonate factories (Zuffa, 1980, 1985; Mount, 1984); (ii) the regime of tidal excursion in macrotidal, mesotidal or microtidal settings (Hayes, 1979); (iii) the relative amplitude of tidal components, and the convergence and divergence of either semi-diurnal or diurnal tides associated with changes in the orbit of the Moon around the Earth (Kvale, 2006); and (iv) the morphological characteristics of the tidally influenced basin (Sztanó & de Boer, 1995; Archer & Hubbard, 2003; Reynaud *et al.*, 2006). This last factor has been little studied until recently, and has virtually been ignored with respect to microtidal environments, where the role of tides in sediment transport generally was assumed to be insignificant.

The strength of tidal currents in a microtidal coastal embayment can be amplified considerably when the length and depth of the bay causes a local amplification of the tidal wave (Pugh, 1987). The Adriatic Sea in the Central Mediterranean represents a present-day analogue where the tidal range is significantly greater than in other areas. Its northern shallow shelf considerably increases the effects of the tidal waves, because a natural oscillation is excited by the Mediterranean tides at the southern entrance, causing diurnal floodings in the Lagoon of Venice with a tidal range up to 1·2 m (Defant, 1961; Storms *et al.*, 2008).

Tidal currents can similarly be amplified within straits linking sea basins with a time-offset build-up of the tidal prism (Allen, 1980, 1984a,b). A modern example is the Messina Strait of southern Italy (Barrier, 1987; Mercier *et al.*, 1987), where the semi-diurnal inversion of the tidal prism in the Tyrrhenian Sea to the north and the Ionian Sea to the south amplifies currents within the strait (Vercelli, 1925; Blanc, 1954). The southward currents descending the sloping floor of the strait reach velocities of 1 to 3 m/sec (Santoro *et al.*, 2002) and form coarse sand dunes

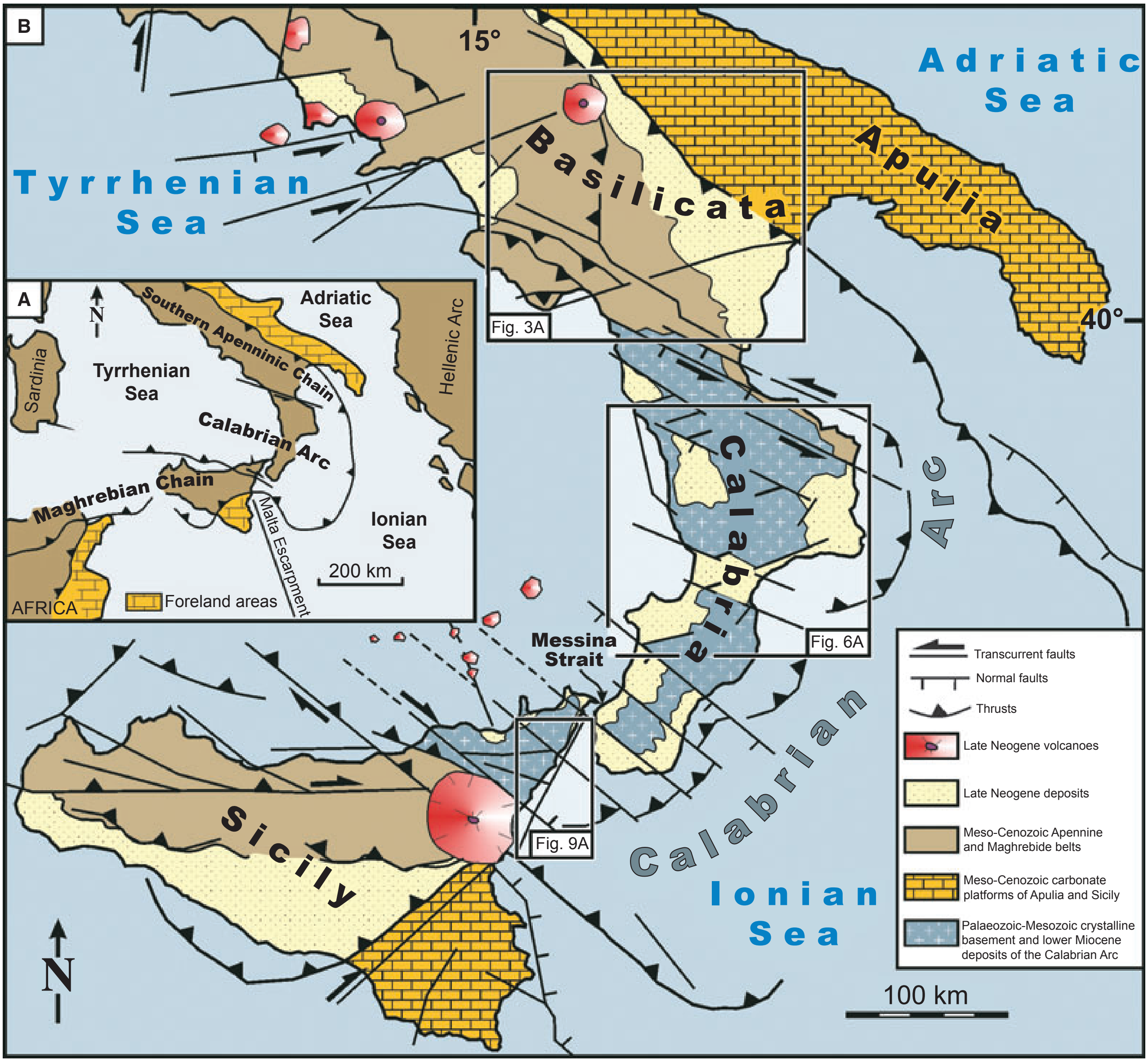

Fig. 1. (A) Geotectonic framework map of the Central Mediterranean, showing the three main orogenic domains of southern Italy: the Apenninic Chain, the Calabrian Arc and the Maghrebian Chain. (B) Simplified geological map of southern Italy, showing the main tectonic lineaments and geodynamic domains. The present study areas are in the regions of Basilicata, Calabria and Sicily (see also Figs 3A, 6A and 9A).

up to 12 m high at sub-littoral to bathyal water depths (Selli *et al.*, 1978; Barrier, 1984; Montenat & Barrier, 1985; Montenat *et al.*, 1987; Colella, 1990, 1996).

A palaeogeographical example of tidalites can be seen in the Central Mediterranean region (Fig. 1A). Since at least the Early Miocene, the region has had a microtidal range of little more than *ca* 35 cm (Wells *et al.*, 2005), with shorelines dominated by waves and wave-generated longshore currents. However, a number of recent sedimentological studies of the Late Cenozoic uplifted palaeo-bays and palaeo-straits in southern Italy (Fig. 1B) have documented tidalites formed by strong tidal currents (Barrier, 1987; Mercier *et al.*, 1987; Colella & D'Alessandro, 1988; Colella, 1995; Longhitano & Nemec, 2005; Nemec *et al.*, 2007; Chiarella & Longhitano, 2008; Messina *et al.*, 2008; Di Stefano & Longhitano, 2009; Longhitano *et al.*, 2010). The local geomorphological settings for tidally dominated sedimentation were controlled by tectonics, and the deposits are mainly sandstones of mixed silici–bioclastic composition, formed during periods when the amplification of tidal currents combined with the presence of cool-water carbonate factories (Colella & Vitale, 1998; Pedley & Grasso, 2002; Capozzi & Picotti, 2003; Roveri & Taviani, 2003; Zecchin *et al.*, 2004; Massari & Chiocci, 2006; Di Stefano & Longhitano, 2007, 2009). The present study reviews and discusses these Plio-Pleistocene tidalites, with a special emphasis on: (i) the relationship between sediment composition and stratification; and (ii) the character of the tidal periodicity record in tectonically controlled microtidal depositional settings.

REGIONAL GEOLOGICAL SETTING

The small basins with Pliocene to Pleistocene tidal sedimentation in southern Italy (Fig. 1B) were open coastal embayments, narrow gulfs and marine straits formed by a combination of tectonic compression and extension in different sectors of the Apenninic Chain and Calabrian Arc, referred to jointly as the southern Italy orogenic belt (Critelli, 1999; Grasso, 2001; Martini *et al.*, 2001; Vai, 2001).

The Apenninic Chain

The Apenninic Chain is an orogenic accretionary wedge (Roure *et al.*, 1991) that presently occupies the Central Mediterranean region (Fig. 1A). It developed as a result of the convergence of the European and African–Adriatic plates, mainly in the Cenozoic (Dewey *et al.*, 1989; Boccaletti *et al.*, 1990; Monaco *et al.*, 1998; Menardi Noguera & Rea, 2000; Grasso, 2001; Patacca & Scandone, 2001). The African foreland includes the continental areas of the Pelagian and Apulian (Adria) blocks, separated since the Jurassic by the opening of the Ionian oceanic basin (Finetti *et al.*, 1996).

The Apenninic Chain consists of various tectonic units derived from the Mesozoic Neotethys ocean and its eastern margin, which today form the regions of Basilicata and Sicily (Fig. 1B). These units were emplaced from adjacent palaeogeographical domains and, from the WSW to the ENE, they are represented by ophiolite oceanic to carbonate platform, to deep-sea basinal successions of Triassic–Cenozoic age. During the orogenic chain construction, these basinal/marginal units experienced compressional deformation and migrated towards a foreland represented by an external crustal block covered with a thick carbonate platform of Late Triassic to Cretaceous age (Fig. 1B; Cello *et al.*, 1989; Lentini *et al.*, 1995; Pescatore *et al.*, 1999; Patacca & Scandone, 2001; Grasso, 2001). During the Miocene to Pliocene, several thrust-top ('piggyback') basins developed in the Apenninic Chain, hosting shallow-water to deep-water sedimentation (Hippolyte *et al.*, 1995). Since the Late Pliocene, some parts of the back-arc zone underwent tectonic extension, which resulted in grabens and coastal embayments with littoral to sub-littoral sedimentation at the eastern periphery of the Tyrrhenian Sea.

The Calabrian Arc

The Calabrian Arc (Fig. 1B) is an arc-shaped zone, thin-skinned thrusting superimposed onto the Apenninic Chain by tectonic accretion (Amodio Morelli *et al.*, 1976; Tortorici, 1982). It consists of a series of ophiolite-bearing tectonic units overlain by basement nappes (Ogniben, 1969). Since the Middle Miocene, the opening of the Tyrrhenian Sea was accompanied by thrusting that caused progressive migration of the Calabrian Arc towards the south-east (Malinverno & Ryan, 1986; Dewey *et al.*, 1989; Decandia *et al.*, 1998). This process involved south-east and ESE-trending strike-slip faults that formed a regional shear zone, dissecting the pre-existing thrust sheets (Fig. 1B; Ghisetti, 1979; Ghisetti & Vezzani, 1981; Rehault *et al.*, 1987; Turco *et al.*, 1990; Knott & Turco, 1991; Monaco & Tansi, 1992; Catalano *et al.*, 1993). The tectonic fragmentation of the Calabrian Arc produced structural highs and marine basins, where littoral to sub-littoral sedimentation took place in the Pliocene to Pleistocene. Strong WNW to ESE tectonic extension occurred in the middle Pleistocene (Cello *et al.*, 1982; Gasparini *et al.*, 1982; Tortorici *et al.*, 1995), with the development of the Calabrian–Sicilian Rift Zone that extends north to south over several tens of kilometres along the coast of western Calabria and eastern Sicily (Monaco *et al.*, 1997; Monaco & Tortorici, 2000; Van Dijk *et al.*, 2000; Tansi *et al.*, 2007). This tectonic development is exemplified by the present-day Messina Strait, which formed as a graben along the axis of a pre-existing, somewhat wider marine strait (Figs 1B and 2; Di Stefano & Longhitano, 2009).

THE TIDALITE-BEARING SUCCESSIONS

The Late Cenozoic shallow-marine deposits of tidally dominated palaeo-bays and palaeo-straits are found in Basilicata, Calabria and Sicily

Fig. 2. Schematic map of southern Italy, showing some of the tidally influenced Late Cenozoic basins in Basilicata, Calabria and Sicily (slightly modified from Longhitano & Nemec, 2005). An inferred Late Pliocene shoreline (dashed line) is indicated for all the tidalite-bearing basins.

(Figs 1B and 2). The sedimentary successions that characterize these three regions are described below, and they have several features in common. The deposits consist of a mixture of siliciclastic and calcareous bioclastic sediment, the former derived from terrigenous river input or from wave abrasion of local bedrock and the latter derived from contemporaneous, foramol-type carbonate factories. Foramol associations or foralgal facies commonly are dominated by non-framework building, light-dependent biota, including benthonic foraminifera, echinoids, molluscs, barnacles, bryozoans and coralline red algae (Lees & Buller, 1972; Pedley & Carannante, 2006; Pomar & Hallock, 2007). The deposits are cross-stratified on a wide range of scales, representing current-produced bedforms from ripples to two-dimensional (2D) dunes up to several metres in thickness. The present study has a comparative regional scope and focuses on small to medium-sized dune cross-strata sets, which are the most common sedimentary structures, showing rhythmic couplets of alternating siliciclastic and bioclastic strata. The descriptive sedimentological terminology used is according to Harms *et al.* (1975, 1982) and Collinson & Thompson (1982).

The Lucanian succession

The north-central segment of the Southern Apennine in Basilicata (Fig. 1B), known as the Lucanian Apennine, contains raised Pliocene shallow-marine deposits in the vicinity of Acerenza, Oppido Lucano and Tricarico (Fig. 3A). The deposits accumulated in small, thrust-top and thrust-front basins during the latest compressional stages of the mountain-chain construction (Pieri *et al.*, 2004; Tropeano *et al.*, 2006; Sabato *et al.*, 2007; Longhitano *et al.*, 2010). The Pliocene succession of the Lucanian Apennine generally consists of two transgressive cyclothems (Ippolito *et al.*, 1975; Bonardi *et al.*, 1988). These units are 200 to 300 m thick, separated by angular unconformities and each showing a transition from terrestrial to fluvial–deltaic and to shoreface and offshore deposits (Pieri *et al.*, 2004). The uppermost unit of Middle to Late Pliocene age is the best-preserved, cropping out in the external zone of the Lucanian Apennine (Fig. 3B; Longhitano, 2008).

The lowest part of this unit consists of basinward-thickening coastal wedges (Fig. 4A) of mixed silici–bioclastic sediment representing shoreface to offshore transition (*sensu* Walker & Plint, 1992) environments (Longhitano *et al.*, 2007; Sabato *et al.*, 2007; Chiarella & Longhitano, 2008). These wedges are organized internally into coarsening-upward bedsets or parasequences (Fig. 4B and C), attributed to a combination of local tectonics, high-frequency relative sea-level changes and hydrodynamics (Chiarella & Longhitano, 2008).

The littoral to sub-littoral sandstones in the parasequences consist of tabular planar cross-strata sets, 10 to 30 cm thick (Fig. 5A and B), showing mainly unidirectional foresets and attributed to the migration of small 2D dunes driven by downwelling tidal currents (cf. Di

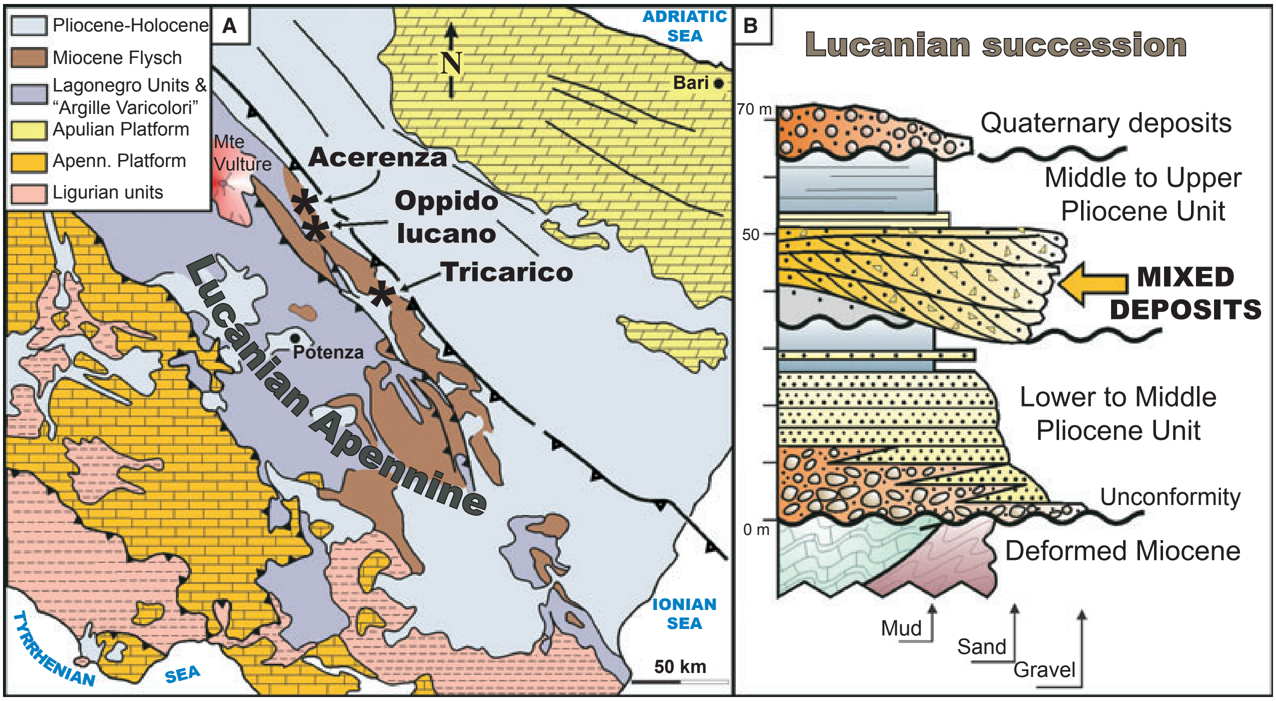

Fig. 3. (A) Geological map of the Lucanian Apennine (modified from Piedilato & Prosser, 2005) showing the main outcrop localities. (B) Generalized stratigraphy of the Neogene to Quaternary sedimentary succession in Basilicata, with the arrow indicating the tidalite-bearing interval (mixed deposits) in the focus of the present study.

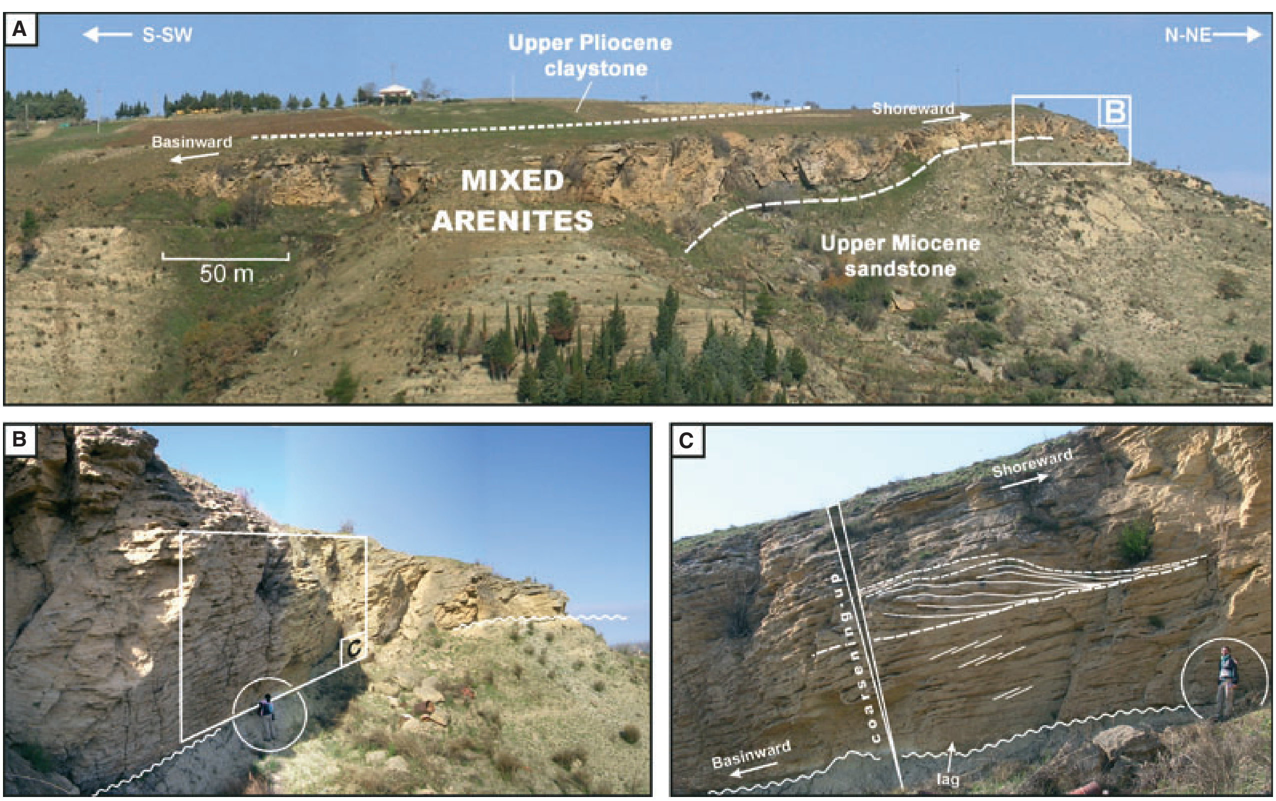

Fig. 4. (A) Panoramic view of an Upper Pliocene coastal wedge of silici–bioclastic deposits, exposed in the vicinity of Acerenza (see locality in Fig. 3A). From right to left, the wedge represents a proximal to distal sublittoral environment. (B) and (C) Details of the proximal part of the clastic wedge, showing a shallowing-upward trend of vertically stacked shoreface deposits. Note the cross-stratified sandstone body encased in planar parallel-stratified shoreface deposits. Person for scale is *ca* 1·8 m tall.

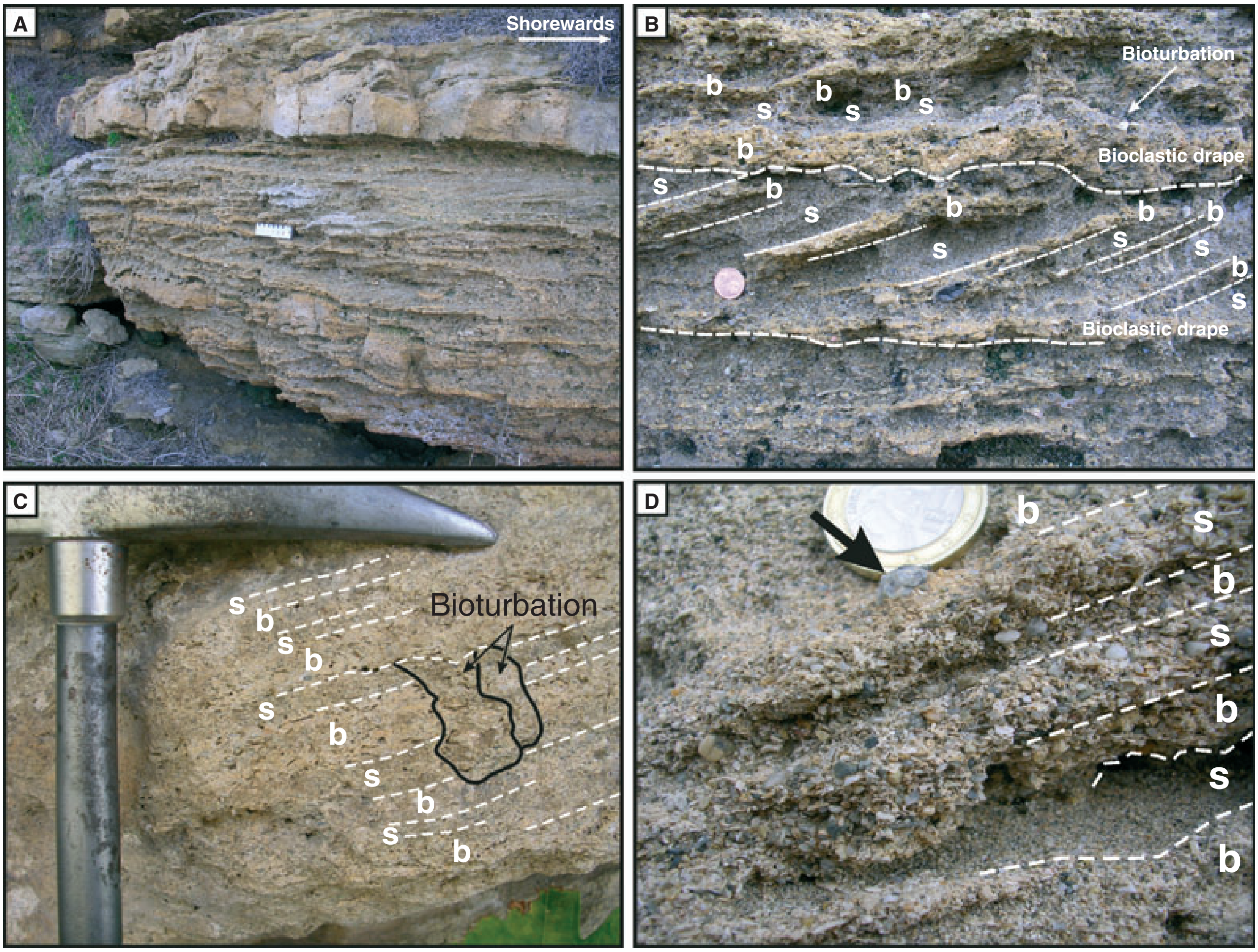

Fig. 5. Tidalites in the Lucanian succession. (A) Tabular cross-stratification in mixed silici–bioclastic deposits (dunes migrate towards the left). The scale is 10 cm long. (B) Dune foreset cross-stratification composed of couplets of thicker siliciclastic 's' and thinner bioclastic 'b' strata (coin is 2·5 cm in diameter). (C) Detail of the previous section, showing the thickness scale of silici–bioclastic 's/b' sediment segregation where laminae are often interrupted by bioturbation. Hammer head is 13 cm long. (D) Detail showing the different rates of segregation of the foreset laminae 's/b'. Note the outsized clast of quartz (arrow; coin is 2·5 cm in diameter).

Stefano *et al.*, 2007; Mateu-Vicens *et al.*, 2008; Di Stefano & Longhitano, 2009; Puga-Bernabéu *et al.*, 2010). The dune foresets show a rhythmic alternation of thicker siliciclastic and thinner bioclastic strata (Fig. 5C and D), with the strata thicknesses and the thicknesses of silici–bioclastic strata couplets varying in a cyclic manner (see quantitative data analysis later in the text).

The Calabrian succession

The Catanzaro and Siderno palaeostraits of Calabria (Fig. 2) are good examples of fault-bounded, tidally dominated seaways that contain Pliocene to Pleistocene deposits. These marine grabens formed along the main tectonic shear zones that dissected the Calabrian Arc during its Neogene eastward translation (Fig. 6A; Van Dijk *et al.*, 2000; Tansi *et al.*, 2007). The narrow, 2 to 3 km wide and 5 to 10 km long seaways linked the Tyrrhenian Sea to the west with the Ionian Sea to the east and were characterized by sub-littoral to bathyal environments with strong tidal currents (Colella & D'Alessandro, 1988; Colella & Longhitano, 1997). Evidence of tidal currents is found also in the Plio–Pleistocene deposits of the Crati Basin and Messina palaeo-strait (Fig. 2) and in the Tortonian sub-littoral calcarenites of the Amantea Basin (Fig. 2; Longhitano & Nemec, 2005).

The Calabrian sedimentary succession in the Catanzaro and Siderno palaeo-straits consists of sandstones and mudstones developed as two transgressive Lower Pliocene to Lower Pleistocene cyclothems (Colella & D'Alessandro, 1988; Cavazza *et al.*, 1997) (Fig. 7A). The silici–bioclas-

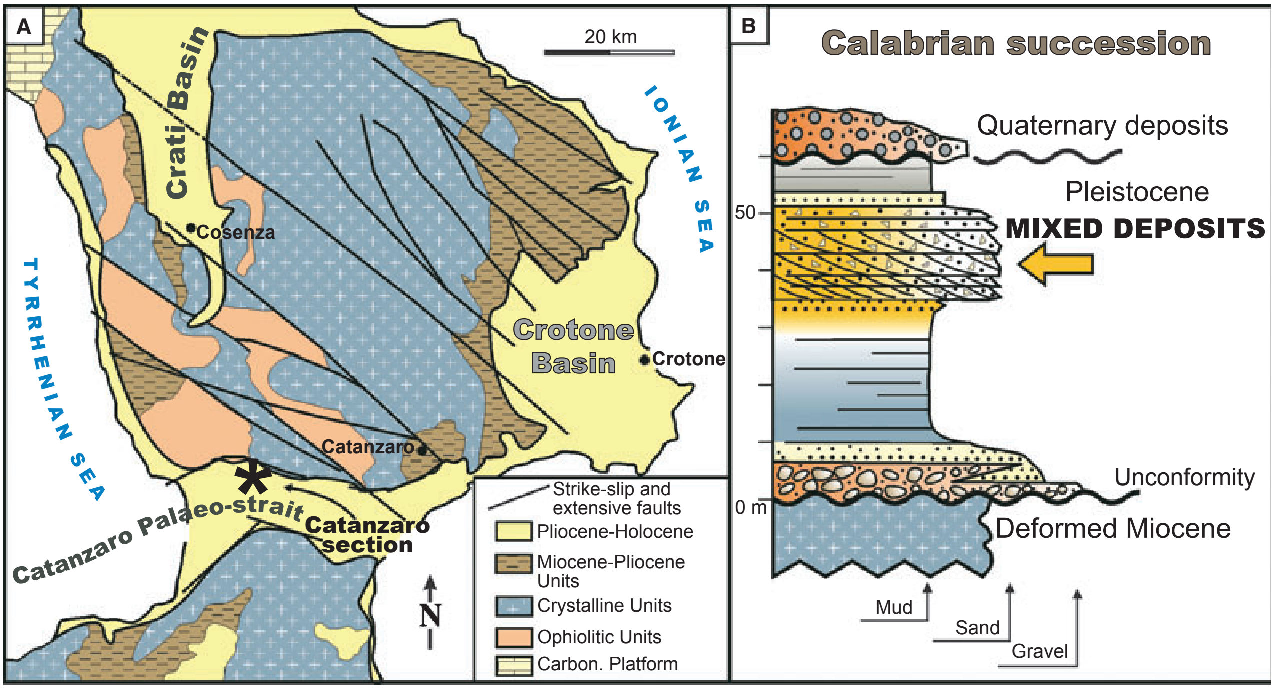

Fig. 6. (A) Simplified geological map of central Calabria (modified from Tansi *et al.*, 2007), showing the location of the outcrop section examined in the present study. (B) Generalized stratigraphy of the Neogene sedimentary succession in Calabria, showing the main unconformity-bounded units; the arrow indicates the tidalite-bearing interval (mixed deposits) in the focus of the present study (see also Fig. 7).

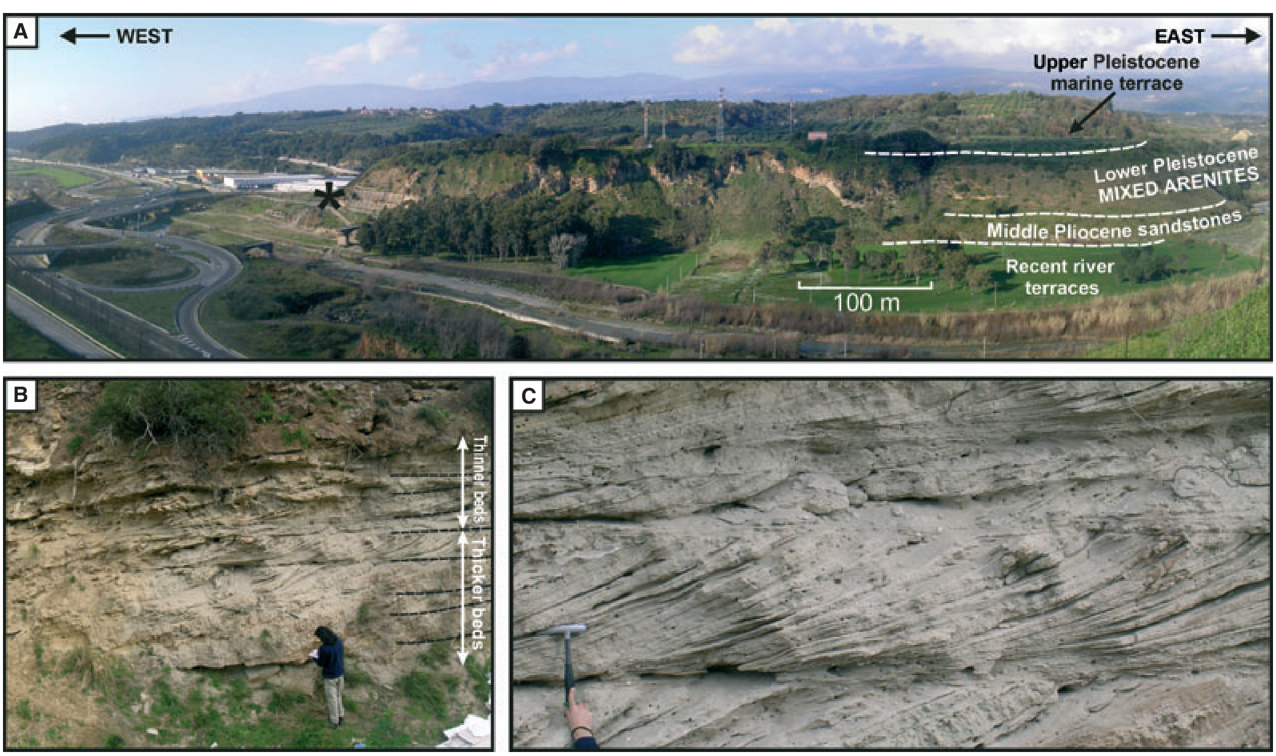

Fig. 7. (A) Panoramic view of the northern margin of the Catanzaro palaeo-strait, where the Plio–Pleistocene marine deposits form the hangingwall of an east-trending normal fault system (the asterisk indicates the studied outcrop). (B) Studied outcrop section showing cross-stratified, unidirectional dunes forming clusters of thicker and thinner strata. Person for scale is *ca* 1·8 m tall. (C) Outcrop detail of tidal deposits (hammer is 35 cm long).

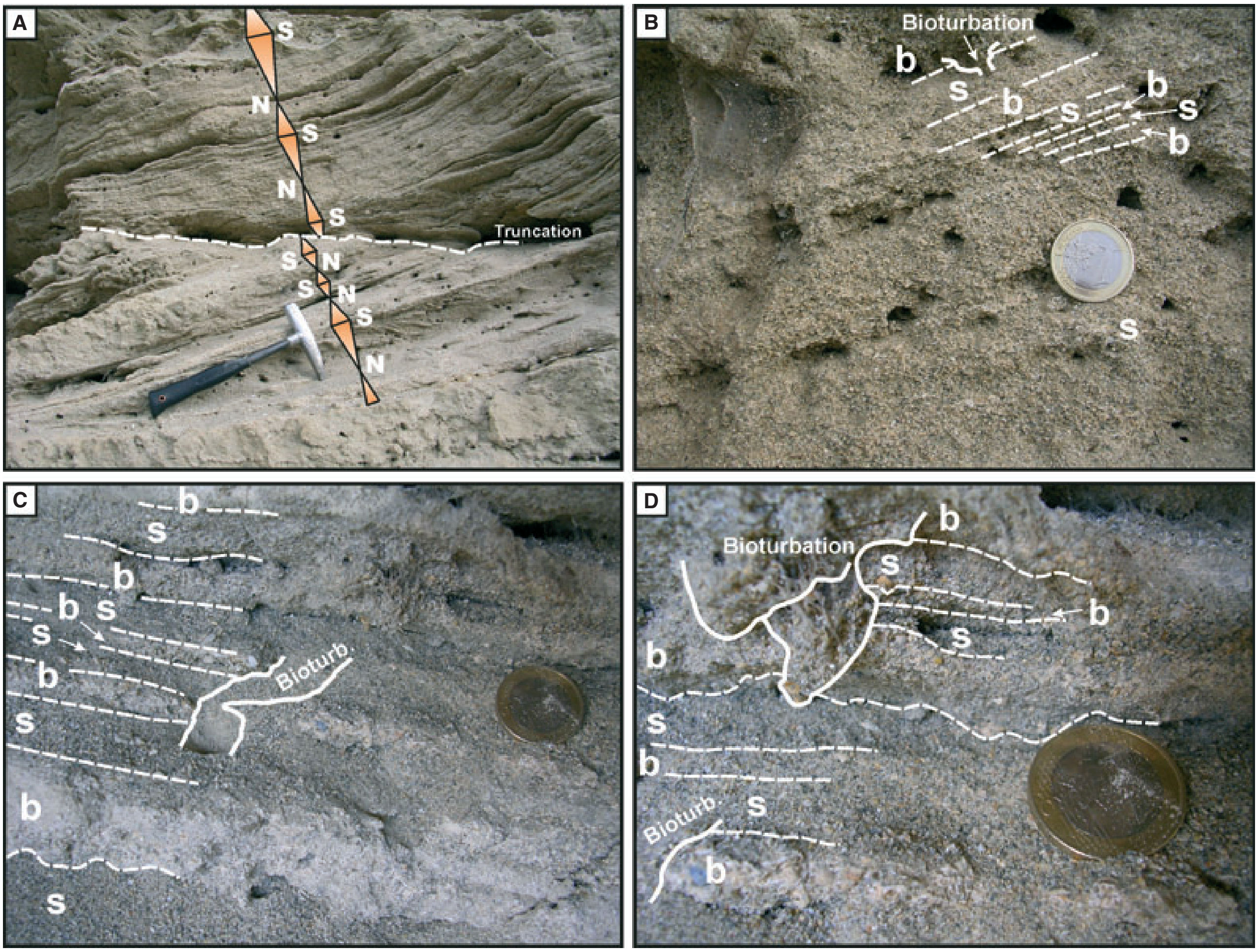

Fig 8. Close-up details from the outcrop shown in Fig. 7B. (A) Dune foreset showing bundled cross-stratification and reflecting neap-spring (N/S) tidal cycles (hammer is 35 cm long). (B) Rhythmic alternation of siliciclastic 's' and bioclastic 'b' strata. (C) and (D) Amalgamated and laterally discontinuous laminae affected by bioturbation. In panels (B), (C) and (D), the coin is 2 cm in diameter.

tic sandstones are characterized by large-scale cross-stratification (Fig. 6B), attributed to the migration of dune bedforms driven by strong and mainly unidirectional tidal currents (Colella & D'Alessandro, 1988).

The tidal sandstones show planar tabular cross-stratification representing small to medium-sized 2D dunes, less than 1 m thick (Fig. 7B), with alternating packages of relatively thick and thin dune cross-sets (Fig. 7C) possibly reflecting high-frequency changes in relative sea-level (cf. Longhitano & Nemec, 2005). The individual dune cross-sets are characterized by strata bundles (Fig. 8A) attributed to the neap-spring tidal cycles (Colella & D'Alessandro, 1988; Colella, 1995; Cavazza *et al.*, 1997; Longhitano & Colella, 1998; Longhitano & Nemec, 2005). Each bundle consists of the rhythmically repeated couplets of alternating siliciclastic and bioclastic strata (Fig. 8B to D) with recognizable cyclic thickness changes.

The Sicilian succession

Marine deposits of a Late Pliocene to Middle Pleistocene age crop out in raised palaeobays on the Ionian and the Tyrrhenian coasts of north-east Sicily (Messina, 2003; Di Stefano *et al.*, 2007; Messina *et al.*, 2008; Di Stefano & Longhitano, 2009), as well as on the Sicilian and Calabrian flanks of the Messina palaeo-strait (Fig. 2). The local coastal embayments formed by the collapse and marine inundation of bedrock fault-blocks in response to regional tectonic extension (Messina *et al.*, 2008). The Messina Strait formed as a tectonic graben along the Siculo-Calabrian rift zone (Monaco & Tortorici, 2000) and originally was broader than it is today, with the Plio–

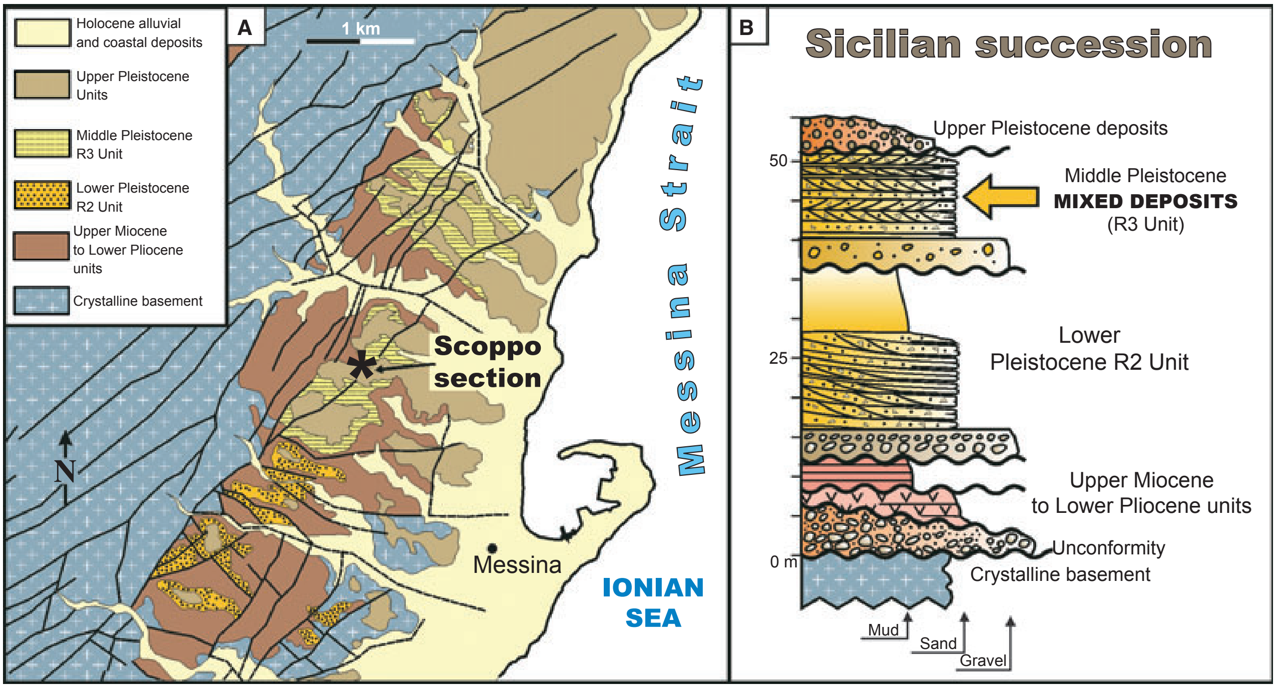

Fig. 9. (A) Geological map of the study area in Sicily, adjacent to the present-day Messina Strait, where the data were collected from the Scoppo outcrop section. (B) Generalized stratigraphy of the marine upper Miocene to Pleistocene succession in northern to eastern Sicily, showing two Pleistocene transgressive cyclothems (R_2 and R_3) and the tidalite-bearing interval studied (arrow); modified from Di Stefano & Longhitano (2009).

Pleistocene sublittoral deposits raised on both flanks of the graben structure (Fig. 9A).

The deposits consist of a variable proportion of siliciclastic and calcareous bioclastic sediment and form three depositional units, locally incomplete, referred to as sequences R_1, R_2 and R_3 (Fig. 9B; Di Stefano *et al.*, 2007). The sequence R_1 consists of laminated clays and rare sandstone layers, whilst the two younger sequences, R_2 and R_3, are dominated by sandstones with ripple cross-lamination and dune-scale (up to 1 m thick) cross-stratification. In the Scoppo section on the Ionian coast of eastern Sicily (Figs 9B and 10A), the tabular planar cross-sets are 10 to 60 cm thick and bidirectional (Fig 10B and C), recording tidal cycles of various temporal periodicities (Di Stefano & Longhitano, 2009). The foreset cross-strata consist of rhythmically repeating couplets of siliciclastic and bioclastic strata (Fig. 11A and B).

Rhythmic silici–bioclastic stratification

A common feature of the Plio–Pleistocene tidal sandstones in the three regions of southern Italy is the abundance of small to medium-sized 2D dune cross-sets, less than 1 m thick, showing rhythmic alternation of siliciclastic and bioclastic foreset strata. The detailed characteristics of this peculiar type of stratification are described and analysed quantitatively below.

Description

The dune cross-strata sets are mainly 10 to 60 cm thick and the strata (foreset) thicknesses range from 1 to 4 cm for siliciclastic sediment and from 0·3 to 2 cm for bioclastic sediment (Figs 5, 8, 10 and 11). The basal contact of cross-strata varies from angular to tangential, but the cross-set boundaries are planar and mainly parallel, tabular. The cross-strata generally are conformable, apart from the occasional surfaces of erosion and reactivation (see Longhitano & Nemec, 2005; Fig. 4B). Many consecutive strata appear to have been amalgamated and are poorly defined, while other strata have been homogenized by bioturbation (Fig. 8C and D). Amalgamation may have occurred principally as a consequence of rapid sediment accumulation, rather than as a diagenetic effect (Einsele *et al.*, 1996), since the primary grain fabric is still recognizable in outcrop.

The siliciclastic strata consist of fine-grained to medium-grained sand, whereas the bioclastic strata show more grain-size variation as the skeletal sand ranges from medium-grained to very coarse-grained. The siliciclastic strata

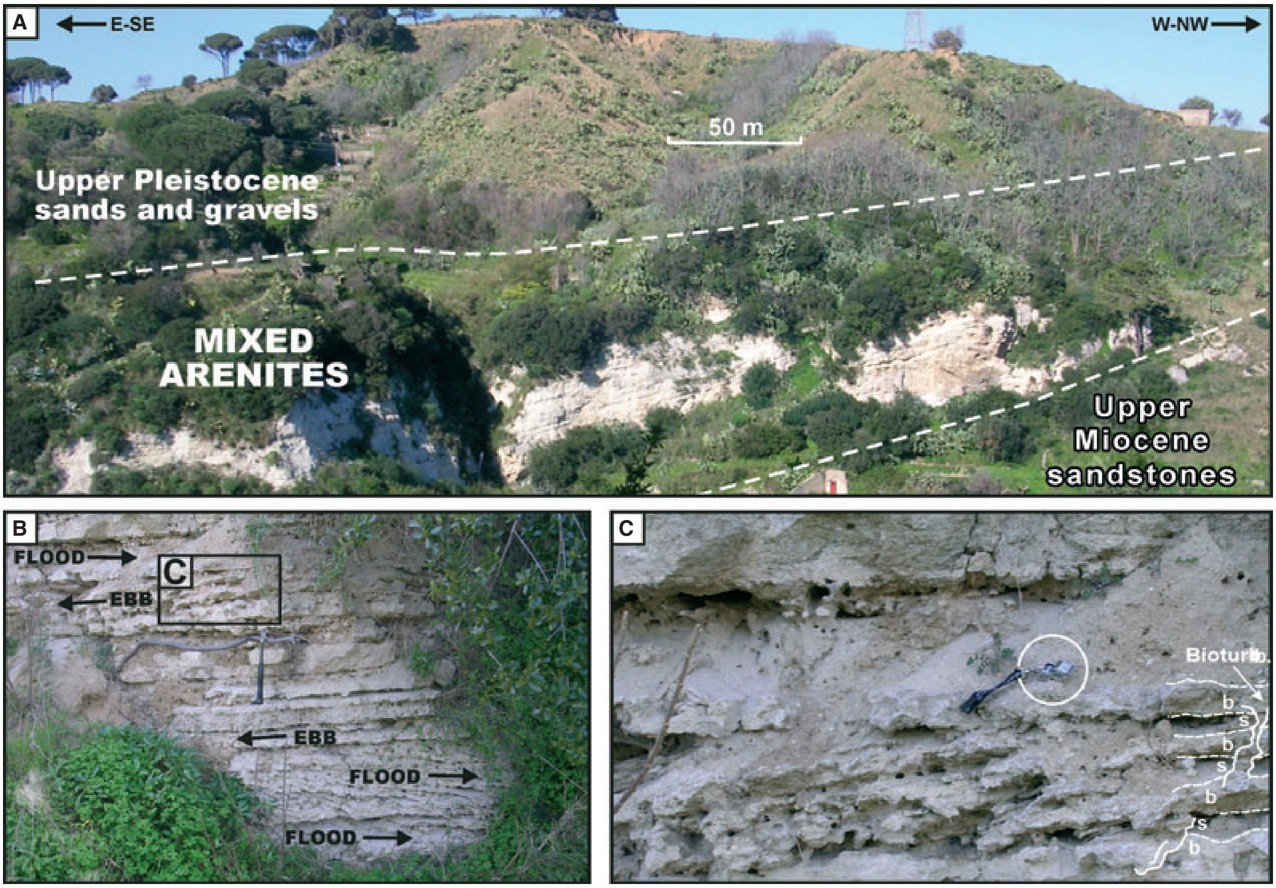

Fig. 10. (A) Mixed deposits of the transgressive cyclothem R_3 cropping out along the Ionian coast of north-eastern Sicily, along the Scoppo section. Here, the tidalite-bearing deposits lie unconformably upon upper Miocene deposits and are overlain by terrigenous upper Pleistocene deposits. (B) Close-up view of the middle-upper interval of the Scoppo outcrop section, showing tabular cross-strata sets with bidirectional foreset directions, representing flood-ebb tidal cycles in the sublittoral zone of the Pleistocene Messina palaeo-strait. (C) Close-up detail of the same outcrop, showing the alternation of siliciclastic and bioclastic foreset strata with diffused bioturbation. The lens for scale is *ca* 5 cm long.

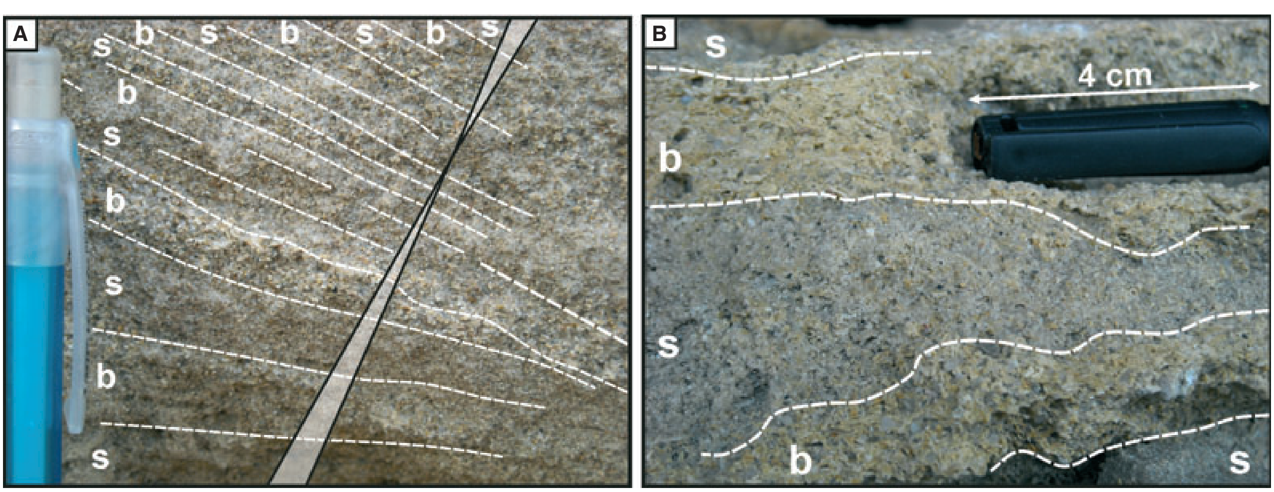

Fig. 11. Close-up details of the Sicilian tidalites shown in Fig. 10B. (A) Dune foreset cross-stratification (palaeocurrent direction to the right) showing rhythmic alternation of bioclastic and siliciclastic strata, composing thinning-up and thickening-up (arrows) lamina sets. (B) Segregated siliciclastic and bioclastic strata. The thickness of bioclastic strata often exceeds that of adjacent siliciclastic strata, because the bioclasts are relatively light fragments of mollusc shells that have a larger dimension if compared with the quartz grains.

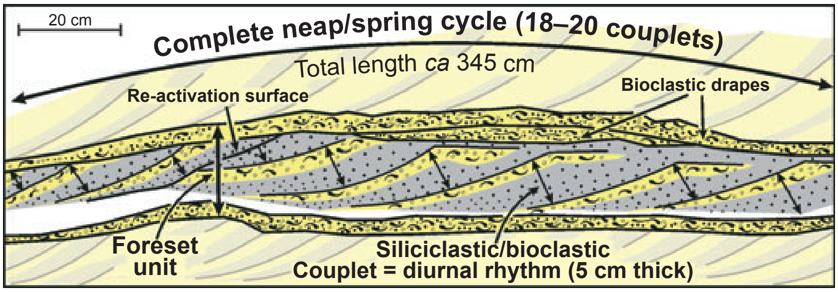

Fig. 12. Field sketch of a well-preserved cross-set of silici–bioclastic strata in the Basilicata section (detail of the outcrop shown in Fig. 5A and B). The cross-sets are unidirectional (palaeocurrent direction to the left). The middle cross-set is underlain and overlain by bioclast-rich strata, which may represent relatively longer periods of decreased hydraulic energy, possibly corresponding to the end of successive synodic monthly cycles (29·53 days).

commonly contain outsized skeletal particles, whereas the bioclastic strata contain a mixture of non-calcareous silt and very fine-grained sand (Fig. 11B). The alternation of the thicker siliciclastic and thinner bioclastic strata forms laterally accreted cyclic rhythmites (*sensu* Reineck & Singh, 1980), although the thickness relationship is reversed locally due to the larger size of shell debris relative to siliciclastic sand grains (Fig. 8B). Of particular interest here is the statistical trend in the thicknesses of strata and of the silici–bioclastic strata couplets in order to disentangle the cyclicity recorded by the cross-strata.

Time-series analysis of strata thicknesses

The measurement of strata thicknesses was limited to foreset intervals with well-preserved and uninterrupted stratification. Seven dune cross-sets were selected from the three successions described in the previous section and were measured along the foreset dip direction, at a constant height above the base of the dune cross-strata set over a lateral distance of 2 to 3 m (Fig. 12). The resulting quantitative datasets are given in Table 1. The presence of cyclicity in such packages of strata should theoretically be detectable by a 'fast' Fourier analysis (Archer, 1994; Archer *et al.*, 1995; Adkins & Eriksson, 1998).

In contrast to similar previous studies (Greb & Archer, 1995; Stupples, 2002), where power spectral analysis (PSA) was applied directly to a raw dataset to detect cyclicity in tidal rhythmite series, the datasets in the present study have first been subjected to a detrending fluctuation analysis (DFA). The DFA technique has proved useful in eliminating apparent trends and revealing true time-series, non-spurious autocorrelation (Granger & Joyeux, 1980; Beran, 1994; Peng *et al.*, 1994). In this approach, the time series to be analysed – containing N data – is first integrated and divided into equal segments containing n data. For each n-long segment, the best-fit least-squares regression line is found to detect the dataset local trend, which may be a first-order or second-order polynomial function. The integrated time series is then detrended by subtracting the local trend-function values from the original data. A detrended time series is expected to show more clearly its inherent cyclicity (sinusoidal), which can then be analysed by the standard PSA technique (Horne & Baliunas, 1986).

The seven measured data series (Table 1) have been analysed using this method and the results are shown in Fig. 13. The plots indicate alternating clusters of thinner and thicker strata, forming a range of depositional cycles (see spectral power peaks in Fig. 13). The highest common frequencies correspond to the spectral values of 0·018, 0·033 and 0·066 cycle/layer, which mean periods of *ca* 55, 30 and 15 layers per cycle, respectively; their possible origin and significance are discussed in the next section.

DISCUSSION

Classical rhythmites in tidal deposits

Cross-stratification generated by tidal marine circulation produces hydraulic bedforms where the height varies with the current strength, sediment availability and temporal persistence (Stride, 1982; Allen, 1984a). Cross-stratification can thus be resolved into descending hierarchical scales within the rock record (Anastas *et al.*, 1997; Longhitano *et al.*, 2010).

In the typical examples of tide-dominated modern and ancient environments, the sedimen-

Table 1. Datasets of cross-strata thickness measurements in seven representative dune foreset units selected in Basilicata, Calabria and Sicily (see plots in Fig. 13).

Bed number	Cross-bed unit 1	2	3	4	5	6	7
1	1·5	**2**	**2·2**	**0·5**	1	0·4	2·2
2	1·5	0·8	1	0·3	**1**	**1·2**	**4**
3	1·4	**0·6**	**1**	**0·5**	1·2	0·8	4·3
4	**0·6**	0·7	0·7	0·2	**0·6**	**1·2**	**2**
5	0·2	**0·8**	**0·5**	**0·4**	1	1·5	1
6	**0·2**	0·8	1·2	0·6	**0·6**	**1**	**1·4**
7	3	0·5	**0·5**	**0·4**	0·8	0·6	1·7
8	1	1·1	**0·7**	0·3	**1**	**1**	**1**
9	**0·8**	**0·7**	0·8	**0·6**	1	0·6	0·5
10	1	1·2	**1**	0·5	**0·8**	**0·4**	**1·8**
11	**0·3**	**1·6**	1·2	**0·8**	1·2	0·7	0·6
12	1	2	**1·8**	0·6	**0·7**	**0·4**	**1**
13	**1**	**1**	1·2	**0·9**	0·8	0·6	1·5
14	1·5	1·5	**1·5**	1	**0·4**	**0·4**	**1**
15	**1·8**	**1·7**	1·8	**0·9**	0·6	0·6	0·7
16	0·4	0·7	**2·2**	0·7	**0·7**	**0·4**	**0·6**
17	**1·2**	**2**	2·5	**0·5**	0·7	0·6	0·5
18	0·8	1	**2·7**	0·6	**0·9**	**0·4**	**0·4**
19	**0·8**	**0·7**	1·3	**0·2**	1·2	0·6	0·6
20	0·8	1	**3**	0·6	**0·8**	**0·4**	**0·4**
21	**2·4**	**0·6**	1·8	**0·8**	1·3	1·1	1·4
22	2·8	1	**1·3**	1·1	**1**	**0·6**	**1**
23	**1·8**	**0·8**	2·8	**0·5**	0·8	1·2	2
24	1·2		**2·3**	0·7	**0·7**	**0·5**	**1**
25	**1·8**		1	0·8	0·6	1·1	2
26	2·5	Covered	**0·8**	**1**	**0·5**	**0·5**	**1**
27	**1·8**	interval	1·1	0·8	0·8	1	1·2
28	2·4		–	**1**	**0·7**	**0·4**	**0·6**
29	**1**		–	0·7	0·7	0·5	1·9
30	2	**1·5**	–	**0·6**	**0·6**	**0·4**	**0·9**
31	**0·8**	2	–	0·8	1	1·2	1·6
32	2·5	**0·8**	–	**0·6**	**0·6**	**1**	**2·5**
33	**1**	0·6	–	0·5	1	0·7	0·5
34	1·3	**0·6**	–	**0·8**	**0·4**	**2·3**	**0·4**
35	–	1	–	0·5	–	0·5	0·4
36	–	**1**	–	**0·4**	–	**1·1**	**0·5**
37	–	0·3	–	0·4	–	1	0·4
38	–	**0·7**	–	**0·3**	–	**2·4**	**0·2**
39	–	0·5	–	0·4	–	0·6	0·2
40	–	**0·8**	–	**0·3**	–	**2·6**	**0·2**
41	–	0·5	–	0·4	–	0·7	0·2
42	–	**0·8**	–	**0·3**	–	**2·5**	**0·5**
43	–	0·6	–	0·4	–	0·5	0·4
44	–	**0·3**	–	**0·3**	–	**2·4**	**0·4**
45	–	0·5	–	0·4	–	0·8	0·3
46	–	**0·3**	–	**0·3**	–	**1·8**	**0·4**
47	–	0·8	–	–	–	0·5	0·3
48	–	**1·2**	–	–	–	**2**	**0·4**
49	–	1·4	–	–	–	0·5	0·3
50	–	**1**	–	–	–	**2**	**0·4**
51	–	0·7	–	–	–	0·5	0·3
52	–	**0·5**	–	–	–	**2**	**0·4**
53	–	0·8	–	–	–	–	2
54	–	–	–	–	–	–	**1**
55	–	–	–	–	–	–	1·7

Table 1. (Continued)

	Cross-bed unit						
Bed number	1	2	3	4	5	6	7
56	–	–	–	–	–	–	**1**
57	–	–	–	–	–	–	2·5
58	–	–	–	–	–	–	**1**
59	–	–	–	–	–	–	2
60	–	–	–	–	–	–	**1·8**
61	–	–	–	–	–	–	2·5
62	–	–	–	–	–	–	**1**
63	–	–	–	–	–	–	1·5
64	–	–	–	–	–	–	**2**
65	–	–	–	–	–	–	1
66	–	–	–	–	–	–	**0·5**
67	–	–	–	–	–	–	1·2
68	–	–	–	–	–	–	**2**
69	–	–	–	–	–	–	1
70	–	–	–	–	–	–	**0·5**
71	–	–	–	–	–	–	1·5
72	–	–	–	–	–	–	**1**
73	–	–	–	–	–	–	2

The thickness values are in centimetres and the boldface values correspond to bioclastic strata.

tary record of a single, dominant tide forms a 'tidal bundle', bounded by reactivation surfaces or mud drapes (Dalrymple, 1992). A classical tidal rhythmite (Visser, 1980) consists of a centimetre-scale cyclical succession of sand and mud laminae, commonly organized into sets representing pure aggradation (i.e. flat-bed vertical accretion) or aggradation combined with progradation (i.e. ripple or dune migration). Ideally, a sandy lamina forms under the maximum current speed of the dominant tide, followed by deposition of a draping mud lamina during the ensuing slack-water phase (Reineck & Singh, 1980). The rhythmic alternation of the couplets of heterolithic laminae thus represents the periodicity record of short-term tidal cycles (Fig. 14A); these may, in turn, form a suite of longer-term cycles according to a specific number of laminae and their thickness characteristics (Kvale & Archer, 1990; Dalrymple *et al.*, 1991; Williams, 1991).

Astronomical tidal cycles include: (i) semidiurnal or diurnal flood-ebb cycles; (ii) half-monthly neap-spring cycles; (iii) semi-annual equinoctial cycles; (iv) 8·8 year lunar apiside cycles; and (v) 18·6 year nodal cycles (Pugh, 1987; de Boer *et al.*, 1989; Archer *et al.*, 1991; Kvale *et al.*, 1995). Each of these cycles can potentially be recorded, depending on the characteristics of the depositional system and on the relative magnitude of the individual forcing factors.

The tidal signal in the sedimentary record can thus potentially be resolved into a range of cycles of different thickness and periodicity scales (Archer *et al.*, 1991; Kvale *et al.*, 1995). In a tidal depositional system, these cycles may all occur concurrently or some may predominate, or a single one may prevail over the others (Allen, 1980, 1984a,b; Dalrymple, 1984; Dalrymple & Makino, 1989; Archer *et al.*, 1991; Kvale & Archer, 1991; Nio & Yang, 1991; Shi, 1991; Archer, 1995, 1998; Tessier, 1998). As a result of various possible disturbances in the system, tidal rhythmite thickness data may be regarded as 'thickness series', rather than a pure 'time series' (Mazumer, 2005).

The observed rhythmic foreset stratification resembles that of the classical tidalites of siliciclastic environments (Visser, 1980; Allen & Homewood, 1984; Greb & Archer, 1995; Mazumder & Arima, 2005), but the lack of mud drapes and the compositional dichotomy of sand cross-strata are significant differences. Furthermore, the power-spectra plots of rhythmite thicknesses (Fig. 13) reveal only short-term cycles. The most recurrent frequencies according to the power spectral value are 0·018, 0·033 and 0·066 cycle/layer; the other minor peaks are considered to be random 'noise' (see the right-hand column of Fig. 13). The three main periodicities correspond to thickness cycles of *ca* 55, 30 and 15 foreset strata (values obtained by inverting the power-

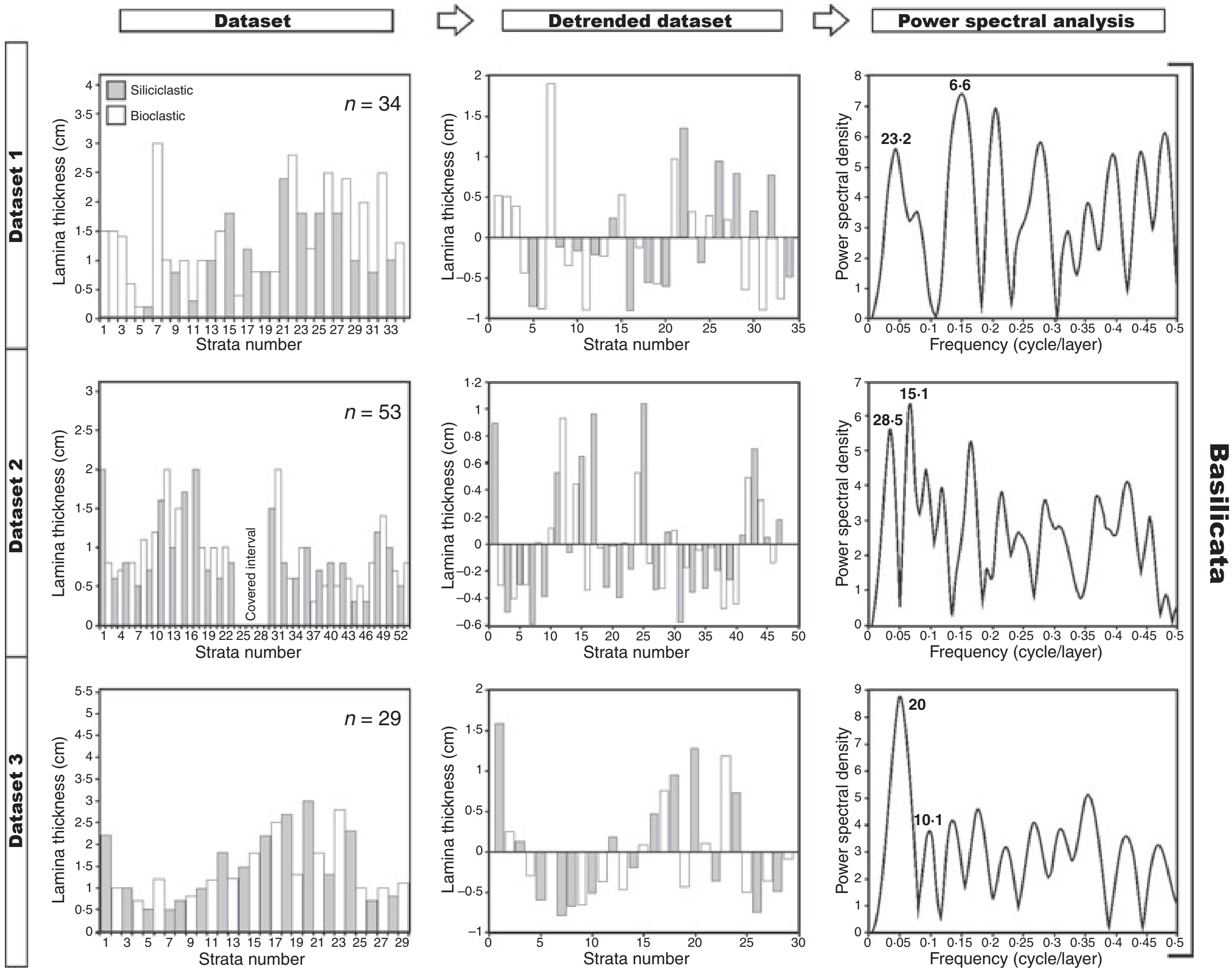

Fig. 13. Plots of the cross-strata thickness datasets from the selected outcrop sites in Basilicata (datasets 1, 2 and 3), Calabria (datasets 4 and 5) and Sicily (datasets 6 and 7), southern Italy (see data in Table 1). The grey and white thickness bars indicate siliciclastic and bioclastic strata, respectively. All the datasets (left-hand column) have been detrended (central column) and analysed with a conventional power-spectral technique (right-hand column). The values in power-spectral plots indicate cycles with the highest power density (period). The irregular low-periodicity frequency peaks are ascribed to a random 'noise' and are disregarded in further analysis.

spectrum frequency values). The most pronounced cycles would then include *ca* 28 (27·5) and 15 tidal bundles, considering that every bundle consists of a pair of strata; one siliciclastic and one bioclastic. The 15-bundle cycles are the strongest, which may indicate a diurnal cyclicity within a pattern of neap-spring tide fluctuations (Adkins & Eriksson, 1998). However, the 28-bundle cycles suggest a weaker, less pronounced signal of semi-diurnal periodicity (Allen, 1981; Allen & Homewood, 1984; Dalrymple, 1992). A combination of diurnal and semi-diurnal cyclicity in the same depositional environment is not expected in a classical tidal system, except for settings characterized by a diurnal inequality (mixed tidal systems). However, these settings usually are macrotidal to mesotidal or highly microtidal, where the discrepancies between two successive high or low tides tend to be well-defined in the sediments. There is little or no possibility of recording diurnal inequalities in a microtidal system where the tidal range is in the order of a few tens of centimetres, such as presently occurs in the Central Mediterranean.

Non-classical tidal rhythmites

As pointed out in the previous section, the tidal cyclicity record in the present case differs significantly from that shown in the classical rhythmites of mud-rich, siliciclastic tidal

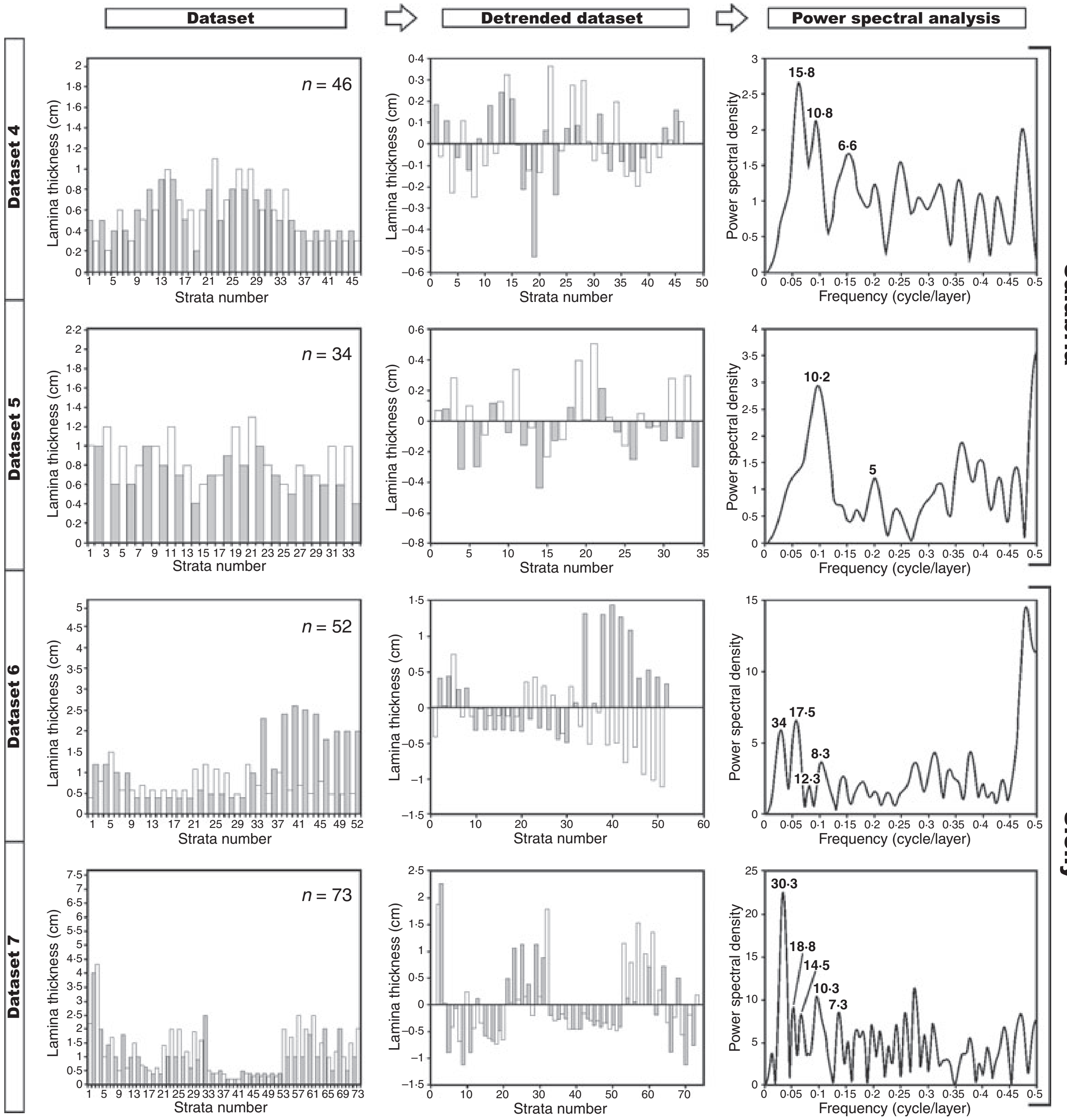

Fig. 13. (continued)

environments. The possible physical causes of the main observed differences are discussed below.

Predominance of short-term cyclicity

The presence of only the shortest-term tidal cycles is known from many ancient environments, where the forcing effect of longer-term factors was virtually muted by the semi-diurnal or diurnal and neap-spring signals (Visser, 1980; Allen, 1981; Allen & Homewood, 1984; Dalrymple, 1992). Such conditions are likely to have occurred in a microtidal setting with the tidal wave enhancement limited to small bays and straits. Since no thicker 'continuous' intervals, uninterrupted by surfaces of truncation and reactivation, have been found during the present study, the possibility of longer-term cycles in these small basins remains to be investigated. There is some evidence that the synodic (monthly) tidal cycles may, at least locally, be recorded in these deposits (Fig. 12).

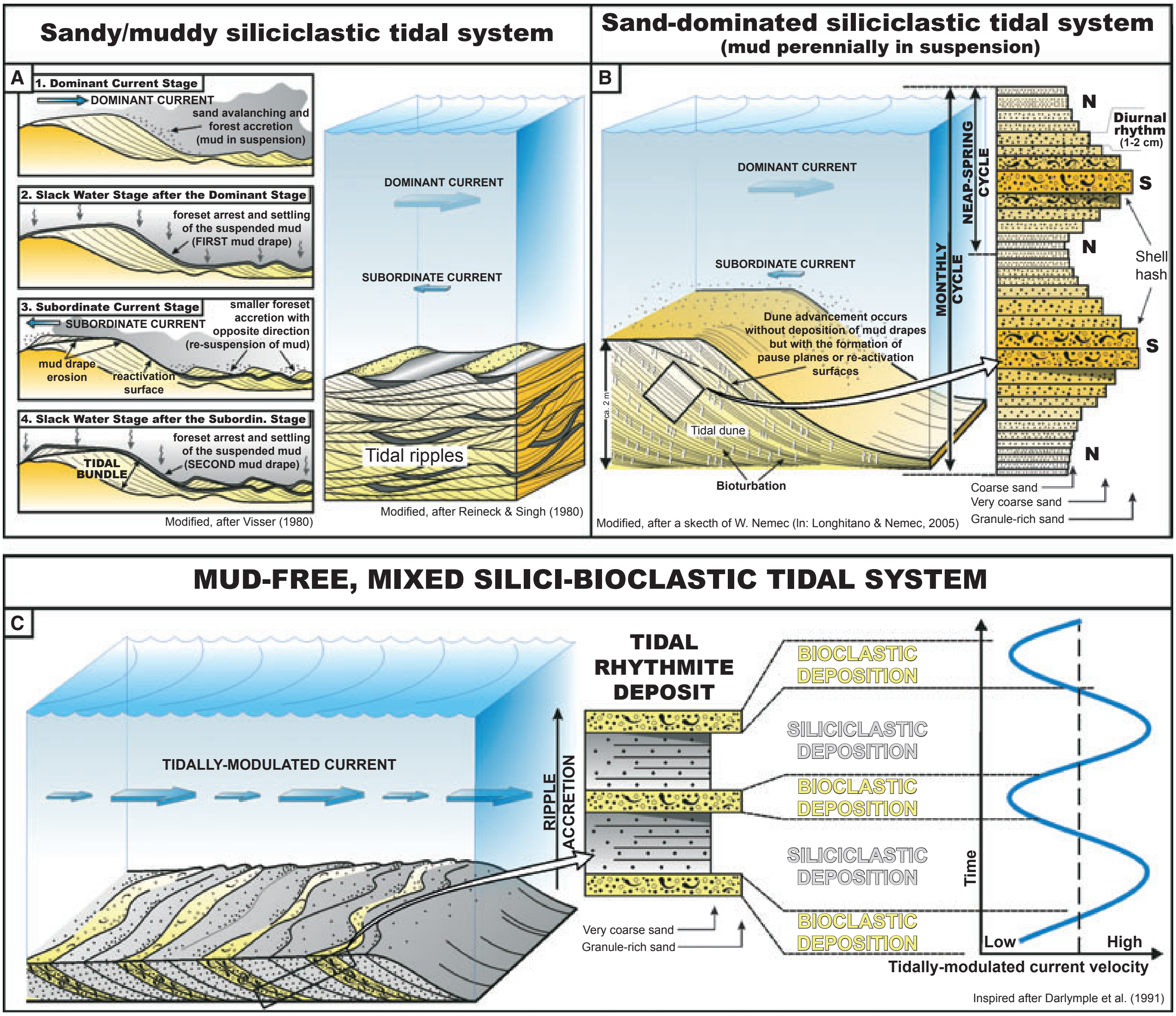

Fig. 14. Comparison of the depositional models for tidal rhythmites. (A) In a classical, mud-bearing siliciclastic tidal system, the deposition under diurnal or semi-diurnal and monthly cycles generates uni-directional or bidirectional cross-stratification with the intervening mud drapes reflecting slack-water phases of tide reversal. (B) In the absence of a mud fraction or its perennial suspension, a sand-dominated system forms bundles of cyclically thicker/coarser and thinner/finer cross-strata, recording neap-spring (N/S) tidal cycles; the shortest-term (diurnal or semi-diurnal) cycles are difficult to recognize. (C) In a sand-dominated, mixed silici–bioclastic system, the tidal rhythmites are characterized by an alternation of siliciclastic and bioclastic cross-strata, as a result of the influence of tidally modulated currents. Bioclastic strata reflect the decline of tidal current competence and hence are comparable in significance to the mud drapes in a classical system; true mud drapes are not deposited because the mud is kept in perennial suspension or is completely absent.

Combined semi-diurnal and diurnal cycles

If the tides are semi-diurnal, a complete neap-spring cycle of 14·77 days will comprise 28 tidal bundles of strata; they may be fewer than 28 if the maximum current speed falls below the threshold for sand movement during the neap tides. The bundles will amount to 14 strata or possibly less if the tides are diurnal. While these cycles can be almost uninterruptedly recorded in sub-tidal environments, they can be discontinuous or incomplete in intertidal settings, where the number of bundles can be much less than theoretically predicted because of the intervention of random disturbances (waves and storms) related to near-shore hydrodynamics (Yang & Nio, 1985; de Boer *et al.*, 1989; Kvale *et al.*, 1999). Irregular departures from the ideal number of bundles for diurnal or semi-diurnal tidal cycles can also be recognized in ancient environments, where they may be attributed to various non-tidal phenomena superimposed on the tidal cyclicity, including the episodic sea storms, significant variations in atmospheric pressure, water salinity, temperature or annual precipitation, as well as short-term relative sea-level changes. All of these non-tidal factors may cause significant 'noise' in the semi-diurnal/diurnal and monthly periodicities of tidal rhythmites (Yang & Nio, 1985; de Boer *et al.*, 1989; Amos *et al.*, 1995; Kvale *et al.*, 1999; Stupples, 2002; Mazumder & Arima, 2005); this might explain the considerable degree of random 'noise' in the power-spectra plots and the apparently diffuse seven or eight bundle cycles in the present example (Fig. 13).

As to the apparent coexistence of semi-diurnal and diurnal cycles in the present case, it is suggested that the two modes, the latter stronger and the former weaker, probably alternate with the neap-spring cycle. Such a pattern characterizes isolated basins with enhanced tidal waves in an overall microtidal setting, probably as a consequence of the sum of different tidal harmonics deriving from the main tidal wave which produced current reflections along the margins of funnel-shaped embayments. Consequently, the diurnal signal in the present case may reflect the main regional mode of tidal-prism oscillations. In palaeo-strait settings, the semi-diurnal signal may derive from the accompanying out-of-phase reversal of the tidal prism in the adjacent parts of the sea connected through narrow passageways. Such a situation is presently observed every six hours in the Tyrrhenian and Ionian sectors of the Central Mediterranean Sea (Montenat *et al.*, 1987). Alternatively, semi-diurnal and diurnal tidal periodicities depicted in the same deposit could have reflected the existence of a diurnal inequality, generated by markedly different amplitudes in two successive high or low tides (Kvale *et al.*, 1995). Such a signal can be difficult to detect in microtidal settings where the tidal range is less than 35 cm as, for example, in the Neogene to Quaternary of the Mediterranean (Wells *et al.*, 2005).

Lack of mud drapes

Many cross-stratified deposits of sand-dominated tidal systems virtually lack interstratal mud drapes and, instead, show a record of short-term tidal cyclicity in the form of bundles of alternating coarser and finer grained sandy strata (Fig. 14 B; cf. Allen & Homewood, 1984; Longhitano & Nemec, 2005; Hampson, 2010; Longhitano *et al.*, 2010). While it is possible that some mud drapes formed and were later eroded, it seems more likely that the mud fraction in these systems was either lacking or kept perennially in suspension. However, the foreset strata of such tidal sand dunes are commonly burrowed (Figs 8C and D, and 10C; Longhitano & Nemec, 2005), which indicates a lower rate of sand deposition (Pollard *et al.*, 1993); this does not necessarily mean stagnant water conditions. The hydraulic energy of the system would decline periodically below the threshold for sand transport, but, depending on the local pattern of 'residual' water circulation, sufficient might still remain to prevent significant mud fallout from suspension.

The microtidal wave in the Mediterranean Sea, when boosted by resonance in a coastal bay or by confinement in a strait, probably retains sufficient residual energy to prevent fully stagnant hydraulic conditions (Pugh, 1987; Messina *et al.*, 2008). For example, the near-bottom mean velocity of a tidal current amplified by confinement in the modern Messina Strait is *ca* 1·3 m/sec at bathyal depth and reaches 3·6 m/sec at the sub-littoral sill (<200 m water depth) in the narrowest part of the strait (Montenat *et al.*, 1987). The sea floor relief and topographic confinement would be quite unlikely to allow such currents to become stagnant during the tide reversal. Indeed, the tidal sand dunes in the modern strait and in the Plio–Pleistocene palaeo-strait record lack mud drapes (Barrier, 1987; Colella & D'Alessandro, 1988; Colella, 1995). Wave action might keep mud in perennial suspension in a tidally dominated littoral environment (Messina & Nemec, 2006) but, as in the southern Italian Plio–Pleistocene basins, the role of waves would be insignificant in a sub-littoral to bathyal range of environments.

Alternatively, in engulfed depositional settings a mud fraction could have been absent, due to a lack of fluvial input to the basin, as documented for the palaeogeographic frame reconstructed in the Lucanian Apennine (cf. Longhitano *et al.*, 2010). The quartz-rich terrigenous fraction abundantly present in these mixed deposits is derived mostly from submarine recycling of older mud-free bedrock (Chiarella & Longhitano, 2008).

Compositional dichotomy of sand strata

The pattern of sediment segregation and the resulting record of tidal cyclicity would be even more complex in a sand-dominated system involving a mixture of siliciclastic and bioclastic sediment, as in the present case of the southern Italian basins. Skeletal detritus, due to its calcitic mineral composition and inherent microporosity, has a relatively low specific density and, hence,

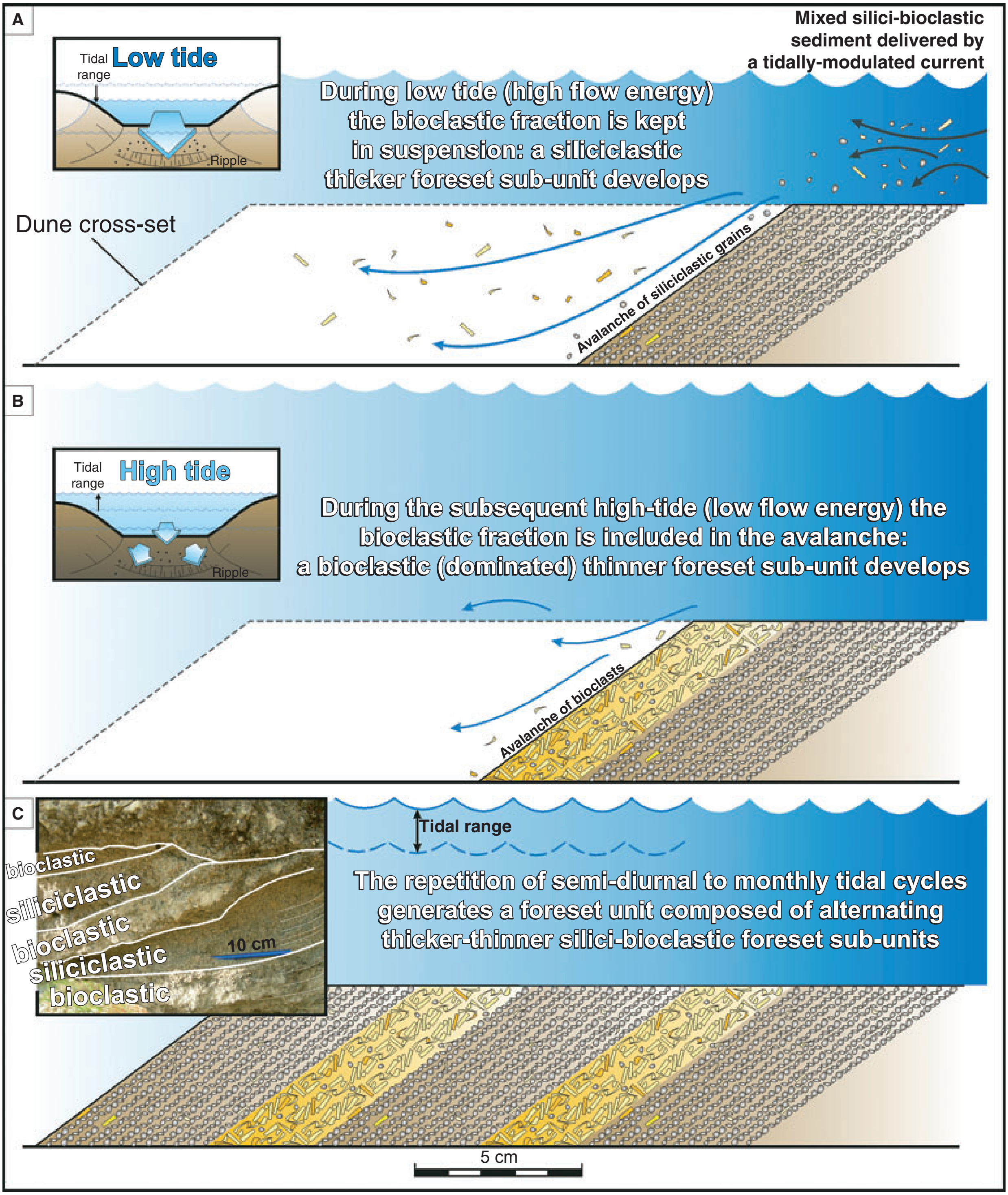

Fig. 15. Hypothetical model for the deposition of a dune foreset made of sediment comprising siliciclastic and bioclastic particles, under a predominant (unidirectional) tidal current subject to semi-diurnal or diurnal cycles (tidally modulated). (A) During the falling tide phase, the reduction of hydraulic cross-section increases bottom shear stresses, whereby a stratum of heavy siliciclastic sediment is deposited from bedload traction, whereas the lighter bioclastic particles are kept in turbulent suspension. (B) During the rising tide phase, the tidal current velocity increases, but is relatively low because of a greater hydraulic cross-section, which favours the tractional deposition of bioclastic sediments and leaves the majority of siliciclastic particles immobile. (C) The repetitive cycles of falling and rising tide generate a non-classical rhythmite composed of the alternating thicker siliciclastic and thinner bioclastic strata; mud is kept perennially in suspension by residual water turbulence and hence, if present, it never forms drapes (modified, from Longhitano *et al.*, 2010).

requires less shear stress to be entrained by current (Maiklem, 1968; Nelson, 1977; Alizai, 1986; Prager *et al.*, 1996). Shell fragments generally are platy in shape, which may further delay their fallout from suspension. Because the density of bioclasts is significantly lower than that of siliciclasts, the hydrodynamic threshold for their motion – for any given particle size – can be expected to be different, resulting in their differential entrainment and segregation (Aigner, 1982; Savarese *et al.*, 1996; Ginsburg, 2005; Jorry *et al.*, 2006; Pomar & Kendall, 2007).

The rhythmical couplets of siliciclastic and bioclastic cross-strata (Fig. 14C) might thus represent, respectively, deposition under the maximum and minimum hydraulic energy of a tidally modulated local circulation pattern (Fig. 15). When the transport competence of the tidal current was at a maximum, the relatively heavy sandy siliciclastic particles, with pebble-sized skeletal debris, were deposited from bedload traction, while the lighter bioclastic particles were kept by the flow in turbulent suspension (Fig. 15A). The deposition of a predominantly bioclastic fraction would occur when the competence of the current declined below the threshold for siliciclastic sand transport (Fig. 15B), although the remnant flow turbulence remained sufficient to prevent any intense fallout of mud. The short-term cyclic repetition of these conditions resulted in the alternation of siliciclastic and bioclastic foreset strata within a migrating dune cross-set (Fig. 15C). The bioclastic strata in this record (Fig. 14C) would then have the same stratigraphic significance as the classical mud drapes in the deposits of mud-rich siliciclastic tidal systems (Nio & Yang, 1991; Archer, 1995, 1998; Stupples, 2002).

Little or no such daily cyclicity might be recorded in a sand-dominated purely siliciclastic or purely bioclastic tidal system, with cross-strata lacking mud drapes (Fig. 14B), unless the available size range of sand grains is sufficiently wide to allow grain-size segregation in a given hydraulic regime of flow-power changes. Otherwise, a sand-dominated purely siliciclastic or bioclastic tidal system would tend to record a longer-term (monthly to yearly) cyclicity.

Marine mixed silici–bioclastic systems have been studied extensively by sedimentologists (Mount, 1984; Mack & James, 1986; Yose & Heller, 1989; Budd & Harris, 1990; Dorsey & Kidwell, 1999; Sanders & Höfling, 2000; D'Alessandro *et al.*, 2004; Wright *et al.*, 2005; Thrana & Talbot, 2006), but little consideration has been given to the hydraulic segregation of sediment fractions of different mineral composition, although the effects of this phenomenon may be important to the resulting sedimentary record (see the discussions of Maiklem, 1968 and Nelson, 1977). The alternating pattern of high and low diurnal or semi-diurnal tides (Fig. 16A), hydraulically 'purified' at sub-littoral depths due to the lack of other significant water movements, will tend to have a characteristic daily impact on a mixed silici–bioclastic tidal system (Southard *et al.*, 1971; Mantz, 1977; Miller & Komar, 1977; Young & Southard, 1978; Young & Mann, 1985; Ghosh *et al.*, 2004). The recognition of a similar pattern of cross-stratification (Fig. 14C) in the stratigraphic record may thus serve as an indicator of the shortest-term tidal periodicity and specific environmental conditions (Fig. 16).

A similar differential style of compositional segregation of the mixed silici–bioclastic sand can be expected in a wave-dominated littoral environment (see Kraus, 1985; and experimental study by Tomkins *et al.*, 2003), although the assemblage of shoreface stratification types will probably be quite different (De Raaf *et al.*, 1977; Driese & Dott, 1984) and the swash-backwash oscillation series will probably have sub-harmonic frequencies (Huntley & Bowen, 1975; Miles & Russel, 2004). Instead of strata-scale segregation, the longer-term fluctuations in wave energy may result in metre-scale intervals of bioclast-rich deposits alternating with similar intervals of siliciclast-dominated deposits (see the 'temporal variability' of Budd & Harris, 1990). These fluctuations will tend to be non-cyclical, as they depend on the local weather conditions, rather than on the astronomical cycles or climatic seasonality alone.

Mixed silici–bioclastic tidal system in isolated bays and straits

The tidally influenced mixed deposits documented in this paper form vertical successions of different thicknesses and architectures that can be referred to as bay-fill and strait-fill successions. In all of the observed sections, a common feature is the record of a rapid transgression at the beginning of the mixed sedimentation and the consequent formation of a basal ravinement surface marked by gravel/shell lags. Mixed deposits are also top-capped by 20 to 30 m of offshore mudstones (Figs 3B, 6B and 9B). Significant cross-stratification occurs in all of the studied examples but, if ripple-scale bedforms prevail in

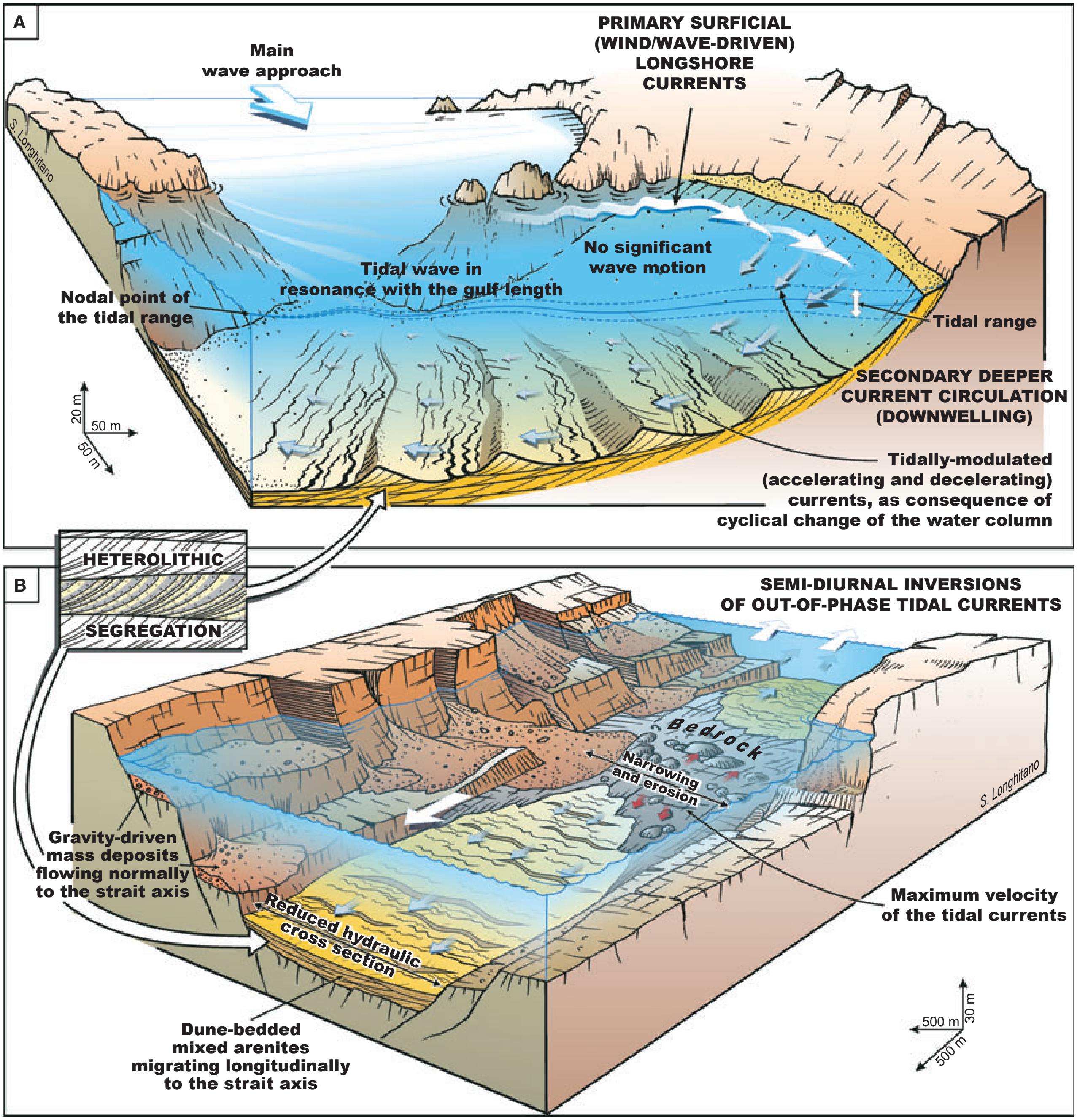

Fig. 16. Comparison between the two main palaeo-geographic scenarios reconstructed to explain the deposition of the tidalite-bearing deposits observed in southern Italy. (A) The confinement of a micro-tidal wave in a coastal embayment may amplify the tidal current waves and maintain the water turbulence at sublittoral depths sufficiently high to keep mud in suspension during the tide reversals. Downwelling, tidally modulated currents would further enhance the turbulence at depth. The cyclic changes in tidal current energy would produce the alternating silici–bioclastic strata in the migrating sand dunes recording short-term, semi-diurnal tidal cycles. (B) In a strait setting, the tidal current amplification occurs in the narrowest cross-section of the strait where erosion prevails. As the strait margins enlarge, the accumulation of mixed sediments organized into large-scale tidal dunes develops into subtidal conditions, as a consequence of decreasing velocity of the tidal currents. Also in this setting, silici–bioclastic strata in the sand dunes recorded tidal cycles of different periodicities under the form of segregation of heterolithic laminae.

bay-fill successions, dunes of larger dimension dominate the deposits filling palaeo-strait settings. These different tidal facies are indicative of two hydrodynamic regimes. (i) Smaller scale bedforms probably reflect marine circulation mostly influenced by weak tidally modulated currents generated in shallow and relatively protected environments. Such sectors were linked to the open sea and consequently were subjected to varying degrees of wave influence (Fig. 16A). (ii) Larger scale dunes may reflect stronger and more steady currents, flowing in deeper environments of marine, tectonically controlled passageways and thus virtually 'protected' from the influence of other additional hydrodynamics, such as waves, storms and other different currents (Fig. 16B).

Shoreface to offshore transitional environments of mixed microtidal, confined coastal areas, are characterized by unidirectional, longshore to offshore directed currents that are responsible for the development of cross-strata that lack mud. As the signal of the dominant waves was mitigated by engulfed morphologies, short-term tidal oscillations represented the dominant hydrodynamics in such areas (Fig. 16A). The geomorphological and hydrodynamic conditions of such basins are fundamental for tidal amplification. As argued by Sztanó & de Boer (1995), the conditions that favour tidal amplification in microtidal settings can be defined as three main types. (i) An amphidromic-type amplification, where the propagating tidal wave in a basin tends to turn around an amphidromic point in an anti-clockwise direction (due to the Coriolis force in the Northern Hemisphere). This condition can be reproduced in basins having a certain width to accommodate a rotary tidal wave (Pugh, 1987). (ii) A resonant-type amplification, where a tidal wave may also be intensified if reflected at the head of an embayment, entering into a state of resonance within the bay. This condition can be fulfilled in long, funnel-shaped embayments (Avoine & Larsonneur, 1987; Kirkby, 1987; Gao *et al.*, 1990; Ke *et al.*, 1996; Plater *et al.*, 2000). (iii) A topographic-type amplification, which is typical of basins with a shallow inshore profile. In these coastal settings, a tidal wave may produce friction with the sea bottom, generating vorticities and residual currents that, if consistent with the order harmonics of basic tidal motions, may amplify tidal excursions in microtidal settings (Stride, 1982; Robinson, 1983; Pugh, 1987; Le Provost, 1991; Parker, 1991).

Some of these conditions of tidal amplification in microtidal settings may also have been reliably realized in the ancient examples discussed in this paper. Mixed deposits of the Lucanian Apennine may arguably have been affected by topographic-induced and/or resonant-induced tidal amplification, rather than the effects of amphidromic-driven phenomena, since coastal embayments were most probably small (*ca* 2 to 3 km long and 0·5 to 1 km wide) and funnel shaped, favouring an increase in the local tidal range. Semi-diurnal oscillations of the water column may have generated tidally modulated downwelling currents responsible for the segregation of the silici–bioclastic deposits accumulating in the sub-littoral environments (Fig. 16A).

On the contrary, in the microtidal straits documented for the Calabrian and Sicilian sectors, tidal amplification occurred due to a reduction in the hydraulic cross-section of the narrowest parts of these marine passageways (Fig. 16B) (Longhitano & Nemec, 2005; Longhitano *et al.*, 2010). In modern analogues, the hydraulic amplification of the tidal currents between two interlinked seas may enhance the effects of bed shear stress in sub-littoral sediments (Colella, 1996). This enhancement produces typical sedimentary structures which record tide-driven bidirectional reverse flows (Allen, 1980, 1984a,b; Dalrymple, 1984; Dalrymple & Makino, 1989; Archer *et al.*, 1991; Kvale & Archer, 1991; Nio & Yang, 1991; Shi, 1991; Archer, 1995, 1998; Tessier, 1998). Large-scale dunes migrating in opposite directions accumulate in specific zones of the strait bottom separated by a bypass area, usually coinciding with the shallowest and narrowest sector of the strait where currents reach their maximum energy, producing erosion rather than deposition (Fig. 16B). These deposits may be interfingered with mass flow deposits derived from adjacent margins and flowing normally to the strait axis (Di Stefano & Longhitano, 2009).

The effect of these conditions in the sedimentary record is observable along the margins of the basins described for the Calabrian and Sicilian sectors, that approximate conditions presently occurring in the Messina Strait in the Central Mediterranean (Fig. 2). Here, the semi-diurnal inversion of tides occurs between the Tyrrhenian Sea to the north and the Ionian Sea to the south (Vercelli, 1925), amplifying descending tidal currents.

Systematic measurements of cross-set thicknesses in outcrop logs and borehole data reveal the 2D-spatial pattern of accumulation of cross-stratified mixed deposits, which is considered to be a crucial element in unravelling reservoir heterogeneity models (Mikes & Bruining, 2006). The volumetric aspect of mixed strata sets is also important because the foresets act as mini-compartments separated by high-angle angular unconformities, textural differences and permeability baffles (Messina *et al.*, 2009). Sandstone permeability parallel to cross-strata is commonly up to four times greater than the permeability normal to cross-strata, and this anisotropy may have a strong effect on the flow of pore fluids, oil recovery and residual oil saturation (Kortekaas, 1985; Hartkamp-Bakker, 1991). This aspect is particularly significant in mixed, well-segregated sediments formed under tidal influence, where the foresets are characterized by a rhythmically changing heterogeneity which can be predicted through time-series analysis, as documented in the present paper.

CONCLUSIONS

The present study has focused on the Pliocene–Pleistocene tidalite-bearing deposits cropping out in a number of peripheral marine basins in Basilicata, western Calabria and northern to eastern Sicily, in southern Italy. The studied basins of the microtidal Mediterranean Sea consisted of coastal embayments and narrow straits, formed by tectonics during the Plio–Pleistocene. Deposition of thick units of cross-stratified, mixed silici–bioclastic sandstone recorded the occurrence of strong tidal currents. Mixed deposits consist of a siliciclastic fraction derived by local bedrock erosion, and of a bioclastic fraction generated from contemporaneous, cool-water foramol-type carbonate factories.

Small to medium-sized (10 to 60 cm thick) two-dimensional dunes with mainly unidirectional foreset dip directions represent the tidalite cross-strata sets investigated in the present study. The Central Mediterranean Sea has had a microtidal range of *ca* 35 cm, and the local amplification of tides is attributed to the enhancement of the tidal wave in some of the bays due to the topographic effects of a shallow inshore profile, as well as to the out-of-phase semi-diurnal reversal of the tidal prism in the narrowest parts of the straits linking the Tyrrhenian and Ionian sectors of the sea.

The tidalites in these peripheral basins differ from the classical tidal rhythmites of mud-bearing siliciclastic tidally influenced depositional systems, because: (i) the foresets consist of alternating strata couplets of segregated siliciclastic and bioclastic sand, lacking classic mud drapes; (ii) the systematic thickness variation of silici–bioclastic strata couplets composing 2 to 3 m long foreset units, statistically analysed with power spectral tests applied on 'detrended' datasets, has pointed out only the shortest-term tidal cycles; and (iii) the diurnal and semi-diurnal tidal cycles represent time-series component patterns of longer-term neap-spring monthly cycles.

The discrepancies between mixed tidal rhythmites and classical rhythmites are attributed to: (i) the specific composition of the tidalite-bearing mixed deposits considered to be more 'sensitive' in recording short-term tidal cycles; and (ii) the specific palaeogeographic setting of a microtidal sea with the tidal currents locally enhanced in its peripheral basins, confined coastal sectors or straits.

These mud-free silici–bioclastic tidal rhythmites, diffusely observable in a number of Pliocene–Pleistocene mixed deposits of the southern Italy orogenic belt, may be considered to be an indicator of the shortest-term tidal cycles and may be diagnostic in recognizing specific tidally dominated depositional environments of confined marine sectors or sub-littoral passageways.

ACKNOWLEDGEMENTS

The study benefited from critical discussions with Dr Marcello Tropeano (Bari University) and Dr Domenico Chiarella (Basilicata University, Italy); the latter kindly offered technical assistance in the field. Dr Giovanni Nico (CNR-IMAA, Bari, Italy) helped with the statistical analysis of quantitative datasets. Prof. Salvatore Critelli (Calabria University, Italy) and Prof. W. Nemec (Bergen University, Norway) critically reviewed and improved an early version of the work. The author is also grateful to Associate Editor, Prof. David Mallinson (East Carolina University, NC, USA), Prof. Cornel Olariu (Jackson School of Geosciences, TX, USA) and an anonymous reviewer, for their fruitful comments and suggestions.

REFERENCES

Adkins, R.M. and **Eriksson, K.A.** (1998) Rhythmic sedimentation in a mid-Pennsylvanian delta-front succession, Magoffin Member (Four Corners Formation, Breathitt Group), eastern Kentucky: a near-complete record of daily, semi-monthly, and monthly tidal periodicities. In: *Tidalites: processes and products* (Eds C.R. Alexander, R.A. Davis and V.J. Henry), *SEPM Spec. Publ.*, **61**, 85–94. Tulsa, OK, USA.

Aigner, T. (1982) Event-stratification in nummulite accumulations and in shell beds from the Eocene of Egypt. In: *Cyclic and Event Stratification* (Eds G. Einsele and A. Seilacher), pp. 248–262. Springer-Verlag, Berlin.

Alexander, C.R., Davis, R.A. and **Henry, V.J.** (1998) Tidalites: Processes and Products. *SEPM Spec. Publ.*, **61**, 171.

Alizai, S.A.K. (1986) Sediment distribution in the intertidal zone of the Tay estuary. *Geol. Bull. Univ. Peshawar*, **19**, 33–46.

Allen, J.R.L. (1980) Sandwaves: a model of origin and internal structure. *Sed. Geol.*, **26**, 281–328.

Allen, J.R.L. (1981) Lower Cretaceous tides revealed by cross-bedding with mud drapes. *Nature*, **289**, 579–581.

Allen, J.R.L. (1984a) *Sedimentary Structures: Their Character and Physical Basis. Developments in Sedimentology*, Vol. 30, unabridged one-volume 2nd edn. Elsevier, Amsterdam, 1256 pp.

Allen, J.R.L. (1984b) *Principles of Physical Sedimentology*. George Allen and Unwin, London, 272 pp.

Allen, P.A. and **Homewood, P.** (1984) Evolution and mechanism of a Miocene tidal sandwave. *Sedimentology*, **31**, 63–81.

Amodio Morelli, L., Bonardi, G., Colonna, V., Dietrich, D., Giunta, G., Ippolito, F., Liguori, V., Lorenzoni, S., Paglionico, A., Perrone, V., Piccarreta, G., Russo, M., Scandone, P., Zanettin Lorenzoni, E. and **Zuppetta, A.** (1976) L'Arco Calabro – Peloritano nell'orogene Appenninico-Maghrebide. *Mem. Soc. Geol. Ital.*, **17**, 1–60.

Amos, C.L., Barrie, J.V. and **Judge, J.T.** (1995) Storm-enhanced sand transport in a microtidal setting, Queen Charlotte Islands, British Columbia, Canada. In: *Tidal Signatures in Modern and Ancient Sediments* (Eds B.W. Flemming and A. Bartholomä), *IAS Spec. Publ.*, **24**, 53–68.

Anastas, A.S., Dalrymple, R.W., James, N.P. and **Nelson, C.S.** (1997) Cross-stratified calcarenites from New Zealand: subaqueous dunes in a cool-water, Oligo-Miocene seaway. *Sedimentology*, **44**, 869–891.

Archer, A.W. (1991) Modeling of tidal rhythmites using modern tidal periodicities and implications for short term sedimentation rates. In: *Sedimentary Modelling: Computer Simulations and Methods for Improved Parameter Definition* (Eds E.K. Franseen, W.L. Kendall and W. Ross), *Kansas Geol. Surv. Bull.*, **223**, 185–194.

Archer, A.W. (1994) Extraction of sedimentological information via computer-based image analysis of gray shale in Carboniferous coal-bearing sections of Indiana and Kansas, USA. *Math. Geol.*, **26**, 47–65.

Archer, A.W. (1995) Modelling of cyclic tidal rhythmites based on a range of diurnal to semi-diurnal tidal-station data. *Mar. Geol.*, **123**, 1–10.

Archer, A.W. (1996) Panthalassa: paleotidal resonance and a global paleocean-seiche. *Palaeoceanography*, **11**, 625–632.

Archer, A.W. (1998) Hierarchy of controls on cyclic rhythmite deposition, Carboniferous basins of eastern and mid-continental USA. In: *Tidalites: Processes and Products* (Eds C.R. Alexander, R.A. Davis and V.J. Henry), *SEPM Spec. Publ.*, **61**, 59–68.

Archer, A.W. and **Hubbard, M.S.** (2003) Highest tides of the world. In: *Extreme Depositional Environments; Mega End Members in Geologic Time* (Eds M.A. Chan and A.W. Archer), *Geol. Soc. Am. Spec. Pap.*, **370**, 151–173.

Archer, A.W., Kvale, E.P. and **Johnson, H.R.** (1991) Analysis of modern equatorial tidal periodicities as a test of information encoded in ancient tidal rhythmites. In: *Clastic Tidal Sedimentology* (Eds D.G. Smith, G.E. Reinson, B.A. Zaitlin and R.A. Rahmani), *Can. Soc. Petrol. Geol. Mem.*, **16**, 189–196.

Archer, A.W., Kuecher, G.J. and **Kvale, E.P.** (1995) The role of tidal-velocity asymmetries in the deposition of silty tidal rhythmites (Carboniferous, Eastern Interior Coal Basin, USA). *J. Sed. Res.*, **A65**, 408–416.

Avoine, J. and **Larsonneur, C.** (1987) Dynamics and behaviour of suspended sediment in macrotidal estuaries along the south coast of the English Channel. *Cont. Shelf Res.*, **7**, 1301–1305.

Barrier, P. (1984) *Evolution tectono-sèdimentaire pliocéne et plèistocene du Detroit de Messine (Italie)*. Thèse Universitaire, Aix-Marseille II, 270 pp.

Barrier, P. (1987) Stratigraphie des dépôts pliocènes et quaternaires du Détroit de Messine. Le Détroit de Messine (Italie). Evolution tectono-sedimentaire récente (Pliocène et Quaternaire) et environment actuel. *Doc. Trav. IGAL (Paris)*, **11**, 59–81.

Beran, J. (1994) *Statistics for Long-Memory Processes*. Chapman & Hall, New York, 144 pp.

Blanc, J.J. (1954) Erosion et sedimentasion littorale actuelle dans le Détroit de Messine. *Bull. Sect. Sci.*, **2**, 11–24.

Boccaletti, M., Ciaranfi, N., Cosentino, D., Deiana, G., Gelati, R., Lentini, F., Massari, F., Moratti, G., Pescatore, T., Ricci Lucchi, F. and **Tortorici, L.** (1990) Palinspastic restoration and paleogeographic reconstruction of the peri-Tyrrhenian area during the Neogene. *Palaeogeogr. Palaeoclimatol. Palaeoecol.*, **77**, 41–50.

de Boer, P.L., Oost, A.P. and **Vissser, M.J.** (1989) The diurnal inequality of the tide as a parameter for recognizing tidal influences. *J. Sed. Petrol.*, **59**, 912–921.

Bonardi, G., D'Argenio, B. and **Perrone, V.** (1988) Geological map of Southern Apennines. *Mem. Soc. Geol. Ital.*, **41**, 1341. Tav. 1.

Budd, D.A. and **Harris, P.M.** (1990) Carbonate-siliciclastic mixtures. *SEPM Reprint Ser.*, **14**, 272.

Capozzi, R. and **Picotti, V.** (2003) Pliocene sequence stratigraphy, climatic trends and sapropel formation in the Northern Apennines (Italy). *Palaeogeogr. Palaeoclimatol. Palaeoecol.*, **190**, 349–371.

Catalano, S., Monaco, C., Tortorici, L. and **Tansi, C.** (1993) Pleistocene strike-slip tectonics in the Lucanian Apennine (southern Italy). *Tectonics*, **12**, 656–665.

Cavazza, W., Blenkinsop, J., De Celles, P.G., Patterson, R.T. and **Reinhardt, E.G.** (1997) Stratigrafia e sedimentologia della sequenza sedimentaria oligocenico-quaternaria del bacino calabro-ionico. *Boll. Soc. Geol. Ital.*, **116**, 51–77.

Cello, G., Guerra, I., Tortorici, L., Turco, E. and **Scarpa, R.** (1982) Geometry of the neotectonic stress field in southern Italy: geological and seismological evidence. *J. Struct. Geol.*, **4**, 385–393.

Cello, G., Tortorici, L., Martini, N. and **Paltrinieri, W.** (1989) Structural styles in the frontal zone of the Southern Apennines, Italy: an example from Molise district. *Tectonics*, **8**, 753–768.

Chan, M.A., Kvale, E.P., Archer, A.W. and **Sonett, C.P.** (1994) Oldest direct evidence of lunar-solar tidal forcing encoded in sedimentary rhythmites, Proterozoic Big Cottonwood Formation, central Utah. *Geology*, **22**, 791–794.

Chiarella, D. and **Longhitano, S.G.** (2008) Sedimentary features of middle-upper Pliocene mixed bioclastic/siliciclastic succession near Acerenza (Lucanian Apennines, southern Italy). In: *Plio-Pleistocene Stratigraphic and Tectonic Evolution of the Southern Italy Foredeep: Key Examples from South Apennines Front and Bradanic Trough (Basilicata Region)* (Eds L. Sabato and M. Tropeano), pp. 69–75. Field Trip Guidebook, GeoSed Congress, Bari.

Choi, K.S. and **Park, Y.A.** (2000) Late Pleistocene silty tidal rhythmites in the macrotidal flat between Youngjong and Yongyou Islands, west coast of Korea. *Mar. Geol.*, **167**, 231–241.

Colella, A. (1990) Active tidal sand waves at bathyal depths observed from submersible and bathysphere (Messina Strait, southern Italy). In: Abstracts, IAS 13th Congress, Nottingham, pp. 98–99.

Colella, A. (1995) Sedimentation, deformational events and eustacy in the perityrrhenian Amantea Basin: preliminary synthesis. *Giorn. Geol.*, **57,** 179–193.

Colella, A. (1996) *I depositi dello Stretto di Messina, un'area ad elevata stabilità ambientale*. Excursion Guidebook, Riunione del Gruppo di Sedimentologia del CNR, Catania, pp. 7–42.

Colella, A. and **D'Alessandro, A.** (1988) Sand waves, Echinocardium traces and their bathyal depositional setting (Monte Torre Palaeostrait, Plio-Pleistocene, southern Italy). *Sedimentology*, **35,** 219–237.

Colella, A. and **Longhitano, S.G.** (1997) *Il Bacino di Amantea: una possibile chiave di lettura della Stretta di Catanzaro*. Atti del Convegno Nazionale GeoItalia, Bellaria, pp. 45–47.

Colella, A. and **Vitale, F.P.** (1998) Eustacy, tectonics and their controls on the depositional patterns of clinostratified shoreface carbonates (late Pliocene, Sicily). In: *Strata and Sequences on Shelves and Slopes* (Ed. A. Colella), pp. 29–69. Excursion Guidebook, SEPM Research Conference, Catania.

Collinson, J.D. and **Thompson, D.B.** (1982) *Sedimentary Structures*. Allen and Unwin, London, 207 pp.

Coughenour, C.L., Archer, A.W. and **Lacovara, K.J.** (2009) Tides, tidalites, and secular changes in the Earth–Moon system. *Earth-Sci. Rev.*, **97,** 59–79.

Critelli, S. (1999) The interplay of lithospheric flexure and thrust accomodation in forming stratigraphic sequences in the southern Apennines foreland basin system, Italy. *Rend. Accad. Nazion. Lincei*, **9,** 257–326.

D'Alessandro, A., Massari, F., Davaud, E. and **Ghibaudo, G.** (2004) Pliocene-Pleistocene sequences bounded by subaerial unconformities within foramol ramp calcarenites and mixed deposits (Salento, SE Italy). *Sed. Geol.*, **166,** 89–144.

Dalrymple, R.W. (1984) The morphology of internal structure of sandwaves in the Bay of Fundy. *Sedimentology*, **31,** 365–382.

Dalrymple, R.W. (1992) Tidal depositional system. In: *Facies Models* (Eds R.G. Walker and N.P. James), pp. 195–218. Geological Association of Canada, St John's.

Dalrymple, R.W. and **Makino, Y.** (1989) Description and genesis of tidal bedding in the Cobequid Bay–Salmon River estuary, Bay of Fundy, Canada. In: *Sedimentary Facies of the Active Plate Margin* (Eds A. Taira and F. Masuda), pp. 151–177. Terra Scientific, Tokyo.

Dalrymple, R.W., Makino, Y. and **Zaitlin, B.A.** (1991) Temporal and spatial patterns of Rhythmite deposition on mud flats in the macrotidal Cobequid Bayã Salmon river estuary, Bay of Fundy, Canada. In: *Clastic Tidal Sedimentology* (Eds D.G. Smith, G.E. Reinson, B.A. Zaitlin and R.A. Rahmani), *Can. Soc. Petrol. Geol. Mem.*, **16,** 137–160.

De Raaf, J.F.M., Boersma, J.R. and **Van Gelder, A.** (1977) Wave-generated structures and sequences from a shallow marine succession, Lower Carboniferous, County Cork, Ireland. *Sedimentology*, **24,** 451–483.

Decandia, F.A., Lazzarotto, A., Liotta, D., Cernobori, L. and **Nicolich, R.** (1998) The CROP03 traverse: insights on post-collisional evolution of Northern Apennines. *Mem. Soc. Geol. Ital.*, **52,** 427–439.

Defant, A. (1961) *Physical Oceanography*. Pergamon Press, Oxford, Vol. 2, 598 pp.

Dewey, J.F., Helman, M.L., Turco, E., Hutton, D.H.W. and **Knott, S.D.** (1989) Kinematics of the western Mediterranean. In: *Alpine Tectonics* (Eds M.P. Coward, D. Dietrich and R.G. Park), *Geol. Soc. London Spec. Publ.*, **45,** 265–283.

Di Stefano, A. and **Longhitano, S.G.** (2007) Sedimentology and biostratigraphy of the lower-middle Pleistocene sedimentary succession of the Ionian Peloritani Mts (NE Sicily). In: Abstracts GeoSed Annual Meeting, Siena, 43 pp.

Di Stefano, A. and **Longhitano, S.G.** (2009) Tectonics and sedimentation of the Lower and Middle Pleistocene mixed bioclastic/siliciclastic sedimentary succession of the Ionian Peloritani Mts (NE Sicily, southern Italy): the onset of the Messina Strait opening. *Centr. Eur. J. Geosci.*, **1,** 33–62.

Di Stefano, A., Longhitano, S.G. and **Smedile, A.** (2007) Sedimentation and tectonics in a steep shallow-marine depositional system: stratigraphic arrangement of the Plio-Pleistocene Rometta succession, NE Sicily (Italy). *Geol. Carpath.*, **58,** 71–87.

Dorsey, R.J. and **Kidwell, S.M.** (1999) Mixed carbonate-siliciclastic sedimentation on a tectonically active margin: example from the Pliocene of Baja California Sur, Mexico. *Geology*, **27,** 10, 935–938.

Driese, S.G. and **Dott Jr, R.H.** (1984) Model for sandstone-carbonate ''cyclothemes'' based on upper member of Morgan Formation (Middle Pensylvanian) of northern Utah and Colorado. *AAPG Bull.*, **68,** 574–597.

Einsele, G., Chough, S.K. and **Shiki, T.** (1996) Depositional events and their records – an introduction. *Sed. Geol.*, **104,** 1–9.

Finetti, I., Lentini, F. and **Carbone, S.** (1996) Il sistema appenninico meridionale-arco calabro-Sicilia: studio geologico-geofisico. *Boll. Soc. Geol. Ital.*, **115,** 529–559.

Flemming, B.W. and **Bartholomä, A.** (1995) Tidal signature in modern and ancient sediments. *IAS Spec. Publ.*, **24,** 358.

Gao, S., Xie, Q. and **Feng, Y.** (1990) Fine-grained sediment transport and sorting by tidal exchange in Xiangshan Bay, Zhejiang, China. *Estuar. Coast. Shelf. Sci.*, **31,** 397–409.

Gasparini, C., Iannacone, G., Scandone, P. and **Scarpa, R.** (1982) Seismotectonics of the Calabrian Arc. *Tectonophysics*, **82,** 267–286.

Ghisetti, F. (1979) Evoluzione neotettonica dei principali sistemi di faglie della Calabria centrale (Neotectonic evolution of main fault systems of Central Calabria). *Boll. Soc. Geol. Ital.*, **98,** 387–430.

Ghisetti, F. and **Vezzani, L.** (1981) Contribution of structural analysis to understanding the geodynamic evolution of the Calabrian Arc (southern Italy). *J. Struct. Geol.*, **3,** 371–381.

Ghosh, S.K., Chakraborty, C. and **Chakraborty, T.** (2004) Combined tide and wave influence on sedimentation of Lower Gondwana coal measures of central India: Barakar Formation (Permian), Satpura Basin. *J. Geol. Soc. London*, **161,** 117–131.

Ginsburg, R. (2005) Disobedient sediments can feedback on their transportation, deposition and geomorphology. *Sed. Geol.*, **175,** 9–18.

Ginsburg, R.N. and **Cunningham, K.J.** (1996) Siliciclastic foundation of South Florida Quaternary carbonates. In: Abstracts 7th International Coral Reef Symposium, Vol. II, 756 pp. International Society for Reef Studies, Panama City.

Granger, C.W.J. and **Joyeux, R.** (1980) An introduction to long-range time series models and fractional differencing. *J. Time Series Anal.*, **1,** 15–30.

Grasso, M. (2001) The Apenninic-Maghrebian orogen in southern Italy, Sicily and adjacent areas. In: *Anatomy of an Orogen: The Apennines and Adjacent Mediterranean*

Basins (Eds G.B. Vai and P.I. Martini), pp. 225–286. Kluwer Academic Publishers, Dordrecht.

Greb, S.F. and **Archer, A.W.** (1995) Rhythmic sedimentation in a mixed tide and wave deposit, Hazel Patch sandstone (Pennsylvanian), eastern Kentucky coal field. *J. Sed. Res.*, **B65,** 96–106.

Greb, S.F. and **Archer, A.W.** (2007) Soft-sediment deformation produced by tides in a meizoseismic area, Turnagain Arm, Alaska. *Geology*, **35,** 435–438.

Guertin, L.A., Missimer, T.M. and **McNeill, D.F.** (2000) Hiatal duration of correlative sequence boundaries from Oligocene-Pliocene mixed carbonate/siliciclastic sediments of the South Florida Platform. *Sed. Geol.*, **134,** 1–26.

Hampson, G.J. (2010) Sediment dispersal and quantitative stratigraphic architecture across an ancient shelf. *Sedimentology*, **57,** 96–141.

Harms, J.C., Southard, J.B., Spearing, D.R. and **Walker, R.G.** (1975) *Depositional Environments as Interpreted from Primary Sedimentary Structures and Stratification Sequences*. SEPM Short Course No. 2 Lecture Notes. Society of Economic Paleontologists and Mineralogists, Dallas, 161 pp.

Harms, J.C., Southard, J.B. and **Walker, R.G.** (1982) *Structures and Sequences in Clastic Rocks*. SEPM Short Course No. 9 Lecture Notes. Society of Economic Paleontologists and Mineralogists, Tulsa, 250 pp.

Hartkamp-Bakker, C.A. (1991) Capillary oil entrapment in cross-bedded sedimentary structures of fluvial sandstone reservoirs. *J. Petrol. Tech.*, **22,** 959–970.

Hayes, M.O. (1979) Barrier island morphology as a function of tidal and wave regime. In: *Barrier Island – from the Gulf of St. Lawrence to the Gulf of Mexico* (Ed. S.P. Latherman), pp. 1–71. Academic Press, New York.

Hippolyte, J.C., Angelier, J. and **Barrier, E.** (1995) Compressional and extentional tectonics in an arc system: example of the southern Apennines. *J. Struc. Geol.*, **17,** 1725–1740.

Horne, J.H. and **Baliunas, S.L.** (1986) A prescription for period analysis of unevenly sampled time series. *Astrophys. J.*, **302,** 757–763.

Huntley, D.A. and **Bowen, A.J.** (1975) Comparison of the hydrodynamics of steep and shallow beaches. In: *Nearshore Sediment Dynamics and Sedimentation* (Eds J. Hails and A. Carr), pp. 69–109. Wiley, London.

Ippolito, F., D'Argenio, B., Pescatore, T. and **Scandone, P.** (1975) Structural-stratigraphic units and tectonic framework of Southern Apennines. In: *Geology of Italy* (Ed. C. Squyres), pp. 317–328. Earth Sciences Society of Lybian Arabian Republic, Tripoli.

Jorry, S.J., Hasler, C.A. and **Davaud, E.** (2006) Hydrodynamic behaviour of Nummulites: implications for depositional models. *Facies*, **52,** 221–235.

Kamp, P.J.J., Harmsen, F.J., Nelson, C.S. and **Boyle, S.F.** (1988) Barnacle-dominated limestone with giant cross-beds in a non-tropical, tide swept, Pliocene forearc seaway, Hawke's Bay, New Zealand. *Sed. Geol.*, **60,** 173–195.

Ke, X., Evans, G. and **Collins, M.B.** (1996) Hydrodynamics and sediment dynamics of The Wash embayment, eastern England. *Sedimentology*, **43,** 157–174.

Kirkby, R. (1987) Introduction: sediment exchanges across the coastal margins of NW Europe. *J. Geol. Soc. London*, **144,** 121–126.

Klein, G.D. (1971) A sedimentary model for determining paleotidal range. *Geol. Soc. Am. Bull.*, **82,** 2585–2592.

Klein, G.D. (1998) Clastic tidalites – a partial retrospective view. In: *Tidalites: Processes and Products* (Eds C.R. Alexander, R.A. Davis and V.J. Henry), *SEPM Spec. Publ.*, **61,** 5–14.

Knott, S.D. and **Turco, E.** (1991) Late Cenozoic kinematics of the Calabrian Arc. *Tectonics*, **10,** 1164–1172.

Kortekaas, Th.F.M. (1985) Water/oil displacement characteristics in cross-bedded reservoir zones. *J. Petrol. Tech.*, **12,** 917–926.

Kraus, N.C. (1985) Field experiments on vertical mixing of sand in the surf zone. *J. Sed. Petrol.*, **55,** 3–14.

Kvale, E.P. (2003) Tides and tidal rhythmites. In: *Encyclopedia of Sediments and Sedimentary Rocks* (Ed. G.V. Middleton), pp. 741–744. Kluwer Academic, Dordrecht, The Netherlands.

Kvale, E.P. (2006) The origin of neap-spring tidal cycles. *Mar. Geol.*, **235,** 5–18.

Kvale, E.P. and **Archer, A.W.** (1990) Tidal deposits associated with low-sulfur coals, Brazil Formation (Lower Pennsylvanian), Indiana. *J. Sed. Petrol.*, **60,** 563–574.

Kvale, E.P. and **Archer, A.W.** (1991) Characteristics of two, Pennsylvanian age, semidiurnal tidal deposits in the Illinois Basin, USA. In: *Clastic Tidal Sedimentology* (Eds D.G. Smith, G.E. Reinson, B.A. Zaitlin and R.A. Rahmani), *Can. Soc. Petrol. Geol. Mem.*, **16,** 179–188.

Kvale, E.P., Archer, A.W. and **Johnsonn, H.R.** (1989) Daily, monthly and yearly tidal cycle within laminated siltstones of the Mansfield Formation (Pennsylvanian) of Indiana. *Geology*, **17,** 365–368.

Kvale, E.P., Cutright, J., Bilodeau, D., Archer, A.W., Johnson, H.R. and **Pickett, B.** (1995) Analysis of modern tides and implications for ancient tidalites. *Cont. Shelf Res.*, **15,** 1921–1943.

Kvale, E.P., Johnson, H.W., Sonett, C.P., Archer, A.W. and **Zawistoski, A.** (1999) Calculating lunar retreat rates using tidal rhythmites. *J. Sed. Res.*, **69,** 1154–1168.

Le Provost, C. (1991) Generation of overtides and compound tides (Review). In: *Tidal Hydrodynamics* (Ed. B.B. Parker), pp. 269–295. John Wiley & Sons, New York.

Lees, A. and **Buller, A.T.** (1972) Modern temperate water and warm water shelf carbonate sediments contrasted. *Mar. Geol.*, **13,** 1767–1773.

Lentini, F., Carbone, S., Catalano, S., Di Stefano, A., Gargano, C., Romeo, M., Strazzulla, S. and **Vinci, G.** (1995) Sedimentary evolution of basins in mobile belts: examples from Tertiary terrigenous sequences of the Peloritani Mts (NE Sicily). *Terra Nova*, **7,** 161–170.

Longhitano, S.G. (2008) Sedimentary facies and sequence stratigraphy of coarse-grained Gilbert-type deltas within the Pliocene thrust-top Potenza Basin (Southern Apennines, Italy). *Sed. Geol.*, **210,** 87–110.

Longhitano, S.G. and **Colella, A.** (1998) *Tettonica transpressiva tortoniana nel Bacino di Amantea (Calabria) e record sedimentario*. Atti della Riunione Annuale del Gruppo di Sedimentologia, Bologna, pp. 45–47.

Longhitano, S.G. and **Nemec, W.** (2005) Statistical analysis of bed-thickness variation in a Tortonian succession of biocalcarenitic tidal dunes, Amantea Basin, Calabria, southern Italy. *Sed. Geol.*, **179,** 195–224.

Longhitano, S.G., Sabato, L. and **Tropeano, M.** (2007) Cross-stratified hybrid arenites from the Pliocene Tricarico succession (southern Apennines): influence of tidal currents and high-frequency relative sea-level changes onto large-scale subaqueous dunes. In: Abstracts GeoSed Annual Meeting, Siena, 55 pp.

Longhitano, S.G., Sabato, L., Tropeano, M. and **Gallicchio, S.** (2010) A mixed bioclastic/siliciclastic flood-tidal delta in a microtidal setting: depositional architectures and hierarchical internal organization (Pliocene, Southern Apennine, Italy). *J. Sed. Res.*, **80,** 36–53.

Lubeseder, S., Redfern, J. and **Boutib, L.** (2009) Mixed siliciclastic-carbonate shelf sedimentation – lower Devonian sequences of the SW Anti-Atlas, Morocco. *Sed. Geol.*, **215,** 1–4, 13–32.

Mack, H.G. and **James, W.C.** (1986) Cyclic sedimentation in the mixed siliciclastic-carbonate Abo-Hueco transitional zone (Lower Permian), southwestern New Mexico. *J. Sed. Res.*, **56,** 635–647.

Maiklem, W.R. (1968) Some hydraulic properties of bioclastic carbonate grains. *Sedimentology*, **10,** 101–109.

Malinverno, A. and **Ryan, W.B.F.** (1986) Extension in the Tyrrhenian Sea and shortening in the Apennines as result of arc migration driven by sinking of the lithosphere. *Tectonics*, **5,** 227–245.

Mantz, P.A. (1977) Incipient transport of fine grains and flakes by fluids – extended Shields diagram. *Proc. Am. Soc. Civ. Eng., J. Hydraul. Div.*, **103,** 601–615.

Martini, P.I., Sagri, M. and **Colella, A.** (2001) Neogene-Quaternary basins of the inner Apennines and Calabrian arc. In: *Anatomy of an Orogen: The Apennines and Adjacent Mediterranean Basins* (Eds G.B. Vai and I.P. Martini), pp. 375–400. Kluwer Academic Publishers, Dordrecht.

Massari, F. and **Chiocci, F.** (2006) Biocalcarenite and mixed cool-water prograding bodies of the Mediterranean Pliocene and Pleistocene: architecture, depositional setting and forcing factors. In: *Cool-Water Carbonates: Depositional Systems and Palaeoenvironmental Controls* (Eds H.M. Pedley and G. Carannante), *Geol. Soc. London Spec. Publ.*, **255,** pp. 95–120.

Mateu-Vicens, G., Pomar, L. and **Tropeano, M.** (2008) Architectural complexity of a carbonate transgressive systems tract induced by basement physiography. *Sedimentology*, **55,** 1815–1848.

Mazumder, R. and **Arima, M.** (2005) Tidal rhythmites and their implications. *Earth-Sci. Rev.*, **69,** 79–95.

Mazumer, R. (2005) Reply to comment of G. Williams on ''Tidal rhythmites and their implications'' by R. Mazumder and M. Arima. *Earth-Sci. Rev.*, **72,** 119–123.

Menardi Noguera, A. and **Rea, G.** (2000) Deep structure of the Campanian-Lucanian Arc (Southern Apennines, Italy). *Tectonophysics*, **324,** 239–265.

Mercier, D., Barrier, P., Beaudoin, B., Didier, S., Montenat, J.L. and **Salinas Zuniga, E.** (1987) Les facteurs hydrodynamiques dans la sédimentazion plio-quaternaire du Détroit de Messine. Le Détroit de Messine (Italie). Evolution tectono-sedimentaire récente (Pliocène et Quaternaire) et environment actuel. *Doc. Trav. IGAL (Paris)*, **11,** 171–183.

Messina, C. (2003) *Il bacino plio-quaternario di Barcellona P.G. (Sicilia nord-orientale): analisi di facies ed evoluzione stratigrafico-sequenziale*. Doctoral dissertation, Catania University, Catania, Italy, 120 pp.

Messina, C. and **Nemec, W.** (2006) *Sedimentological and statistical analysis of the Garn Formation in the Kristin field.* Report to Statoil Research Centre, Trondheim, 82 pp.

Messina, C., Rosso, A., Sciuto, F., Di Geronimo, I., Nemec, W., Di Dio, T., Di Geronimo, R., Maniscalco, R. and **Sanfilippo, R.** (2008) Anatomy of a transgressive systems tract revealed by integrated sedimentological and palaeoecological study: the Barcellona P.G. Basin, northeastern Sicily, Italy. In: *Sedimentary Processes, Environments and Basins – A Tribute to Peter Friend* (Eds G. Nichols, C. Paola and E.A. Williams), *IAS Spec. Publ.*, **38,** 367–399.

Messina, C., Nemec, W. and **Longhitano, S.** (2009) Statistical properties of tidal dunes and their use in reservoir modelling. In: Abstracts IAS Annual Meeting, Alghero, 55 pp.

Meyer, R. and **Krauser, F.F.** (1998) Unconformities within a progradational estuarine system: the Upper Santonian Virgelle Member, Milk River Formation, Writing-on-stone Provincial Park, Alberta, Canada. In: *Tidalites: Processes and Products* (Eds C.R. Alexander, R.A. Davis and V.J. Henry), *SEPM Spec. Publ.*, **61,** 129–141.

Mikes, D. and **Bruining, J.** (2006) Standard flow cells to incorporate small-scale heterogeneity (crossbedding) in a reservoir model. *Mar. Petrol. Geol.*, **23,** 979–993.

Miles, J.R. and **Russel, P.E.** (2004) Dynamics of reflective beach with a low tide terrace. *Cont. Shelf Res.*, **24,** 1219–1247.

Miller, M.C. and **Komar, P.D.** (1977) The development of sediment threshold curves for unusual environments (Mars) and for inadequately studied materials (foram sands). *Sedimentology*, **24,** 709–721.

Monaco, C. and **Tansi, C.** (1992) Strutture transpressive lungo la zona trascorrente sinistra nel versante orientale del Pollino (Appennino calabro-lucano) (Transpressional structures along the left-lateral strike-slip zone on the eastern slope of Mt. Pollino (Calabrian-Lucanian Apennine)). *Boll. Soc. Geol. Ital.*, **111,** 291–301.

Monaco, C. and **Tortorici, L.** (2000) Active faulting in the Calabrian Arc and eastern Sicily. *J. Geodyn.*, **29,** 407–424.

Monaco, C., Tapponnier, P., Tortorici, L. and **Gillot, P.Y.** (1997) Late Quaternary slip rates on the Acireale-Piedimonte normal faults and tectonic origin of Mt. Etna (Sicily). *Earth Planet. Sci. Lett.*, **147,** 125–139.

Monaco, C., Tortorici, L. and **Paltrinieri, W.** (1998) Structural evolution of the Southern Apennines, southern Italy. *J. Struct. Geol.*, **20,** 617–638.

Montenat, C. and **Barrier, P.** (1985) Géodynamique des seuils et des hauts-fonds. *Bull. Sect. Sci.*, **9,** 11–24.

Montenat, C., Barrier, P. and **Di Geronimo, I.** (1987) The Strait of Messina, past and present: a review. *Doc. Trav. IGAL (Paris)*, **11,** 7–13.

Mount, J.F. (1984) Mixing of siliciclastic and carbonate sediments in shallow shelf environments. *Geology*, **12,** 432–435.

Nelson, C.S. (1977) Grain-size parameters of insoluble residues in mixed terrigenous-skeletal carbonate sediments and sedimentary rocks: some New Zealand examples. *Sedimentology*, **24,** 31–52.

Nemec, W., Longhitano, S.G. and **Messina, C.** (2007) Statistical properties of tidal dune complexes. In: Abstracts British Sedimentological Research Group Annual Meeting, Birmingham University, Birmingham, UK, pp. 45–46.

Nio, S.D. and **Yang, C.S.** (1991) Diagnostic attributes of clastic tidal deposits: a review. In: *Clastic Tidal Sedimentology* (Eds D.G. Smith, G.E. Reinson, B.A. Zaitlin and R.A. Rahmani), *Can. Soc. Petrol. Geol. Mem.*, **16,** 3–28.

Ogniben, L. (1969) Schema introduttivo alla geologia del confine calabro-lucano (Introductory scheme to the geology of the Calabrian-Lucanian boundary). *Mem. Soc. Geol. Ital.*, **8,** 453–763.

Parker, B.B. (1991) The relative importance of the various nonlinear mechanisms in a wide range of tidal interactions (Review). In: *Tidal Hydrodynamics* (Ed. B.B. Parker), pp. 237–268. John Wiley & Sons, New York.

Patacca, E. and **Scandone, P.** (2001) Late thrust propagation and sedimentary response in the thrust-belt-foredeep system of the Southern Apennines (Pliocene-Pleistocene).

In: *Anatomy of an Orogen: The Apennines and the Adjacent Mediterranean Basins* (Eds G.B. Vai and I.P. Martini), pp. 401–440. Kluwer Academic Publishers, Dordrecht.

Pedley, M. and **Carannante, G.** (2006) Cool-water carbonate ramps: a review. In: *Cool-Water Carbonates: Depositional Systems and Palaeoenvironmental Controls* (Eds H.M. Pedley and G. Carannante), *Geol. Soc. London Spec. Publ.*, **255,** 1–9.

Pedley, M. and **Grasso, M.** (2002) Lithofacies modelling and sequence stratigraphy in microtidal cool-water carbonates: a case study from the Pleistocene of Sicily, Italy. *Sedimentology*, **49,** 533–553.

Peng, C.K., Buldyrev, S.V., Havlin, S., Simons, M., Stanley, H.E. and **Goldberger, A.L.** (1994) Mosaic organization of DNA nucleotides. *Phys. Rev.*, **49,** 1685–1689.

Pescatore, T., Renda, P., Schiattarella, M. and **Tramutoli, M.** (1999) Stratigraphic and structural relationships between Meso-Cenozoic Lagonegro basin and coeval carbonate platforms in southern Apennines, Italy. *Tectonophysics*, **315,** 269–286.

Piedilato, S. and **Prosser, G.** (2005) Thrust sequences and evolution of the external sector of a fold and thrust belt: an example from the Southern Apennines (Italy). *J. Geodyn.*, **39,** 386–402.

Pieri, P., Sabato, L., Tropeano, M., Gallicchio, S., Loiacono, F. and **Schiattarella, M.** (2004) Plio-Pleistocene stratigraphic and tectonic evolution of the foreland-foredeep-chain system in southern Italy. Excursion Guidebook, 32nd GeoItalia International Geological Congress, Florence, Italy, Vol. 4 (P14-P36), pp. 1–48.

Plater, A.J., Ridgway, J., Rayner, B., Shennan, I., Horton, B.P., Haworth, E.Y., Wright, M.R., Rutherford, M.M. and **Wintle, A.G.** (2000) Sediment provenance and flux in the Tees Estuary: the record from the Late Devensian to the present. In: *Holocene Land-Ocean Interaction and Environmental Change Around the North Sea* (Eds I. Shennan and J. Andrews), *Geol. Soc. Publ. House, Bath, Spec. Publ.*, **166,** 171–195.

Pollard, J.E., Goldring, R. and **Buck, S.G.** (1993) Ichnofabrics containing Ophiomorpha: significance in shallow water facies interpretation. *J. Geol. Soc. London*, **150,** 149–164.

Pomar, L. and **Hallock, P.** (2008) Carbonate factories: a conundrum in sedimentary geology. *Earth-Sci. Rev.*, **87,** 134–169.

Pomar, L. and **Kendall, C.G.St.C.** (2007) Architecture of carbonate platforms: a response to hydrodynamics and evolving ecology. In: *Controls on Carbonate Platform and Reef Development* (Eds J. Lukasik and A. Simo), *SEPM Spec. Publ.*, **89,** 187–216.

Prager, E.J., Southard, J.B. and **Vivoni-Gallart, E.R.** (1996) Experiments on the entrainment threshold of well-sorted and poorly sorted carbonate sands. *Sedimentology*, **43,** 33–40.

Puga-Bernabéu, A., Martín, J.M., Braga, J.C. and **Sánches-Almazo, I.M.** (2010) Downslope-migrating sandwaves and platform-margin clinoforms in a current-dominated, distally steepened temperate-carbonate ramp (Guadix Basin, Southern Spain). *Sedimentology*, **57,** 293–311.

Pugh, D.T. (1987) *Tides, Surges and Mean Sea-Level*. John Wiley and Sons, Chichester, 472 pp.

Rehault, J.P., Moussat, E. and **Fabbri, A.** (1987) Structural evolution of the Tyrrhenian back-arc basin. *Mar. Geol.*, **74,** 123–150.

Reineck, H.E. and **Singh, I.B.** (1975) *Depositional Sedimentary Environments, with Reference to Terrigenous Clastics*. Springer-Verlag, New York, 439 pp.

Reineck, H.E. and **Singh, I.B.** (1980) *Depositional Sedimentary Environments*. Springer-Verlag, Berlin, 551 pp.

Reynaud, J.-Y., Dalrymple, R.W., Vennin, E., Parize, O., Besson, D. and **Rubino, J.-L.** (2006) Topographic controls on production and deposition of tidal cool-water carbonates, Uzès Basin, SE France. *J. Sed. Res.*, **76,** 117–130.

Robinson, I.S. (1983) Tidally induced residual flows. In: *Physical Oceanography of Coastal and Shelf Seas* (Ed. B. Johns), pp. 321–356. Elsevier, Amsterdam.

Roep, T.B. (1991) Neap-spring cycles in a subrecent tidal channel fill (3665 BP) at Schoorldam, NW Netherlands. *Sed. Geol.*, **71,** 213–230.

Roure, F., Casero, P. and **Vially, R.** (1991) Growth processes and melanges formation in the southern Apennines accretionary wedge. *Earth Planet. Sci. Lett.*, **102,** 395–412.

Roveri, M. and **Taviani, M.** (2003) Calcarenite and sapropel deposition in the Mediterranean Pliocene: shallow- and deep-water record of astronomically driven climatic events. *Terra Nova*, **15,** 279–286.

Sabato, L., Longhitano, S.G., Tropeano, M., Gallicchio, S. and **Pieri, P.** (2007) Complex stratigraphic patterns in the Pliocene wedge-top hybrid succession of Tricarico (Southern Apennines, Italy). In: Abstracts 25th IAS Meeting of Sedimentology, Patras, 302 pp.

Sanders, D. and **Höfling, R.** (2000) Carbonate deposition in mixed siliciclastic-carbonate environments on top of an orogenic wedge (Late Cretaceous, Northern Calcareous Alps, Austria). *Sed. Geol.*, **137,** 127–146.

Santoro, V.C., Amore, E., Cavallaro, L., Cozzo, G. and **Foti, E.** (2002) Sand waves in the Messina Strait, Italy. *J. Coast. Res.*, **36,** 640–653.

Savarese, M., Dodd, J.R. and **Lane, N.G.** (1996) Taphonomic and sedimentological implications of crinoid intraskeletal porosity. *Lethaia*, **29,** 141–156.

Selli, R., Colantoni, P., Fabbri, A., Rossi, S., Borsetti, A.M. and **Gallignani, P.** (1978) Marine geological investigation on the Messina Strait and its approaches. *Giorn. Geol.*, **42,** 2, 1–70.

Shi, Z. (1991) Tidal bedding and tidal cyclicities within the intertidal sediments of a microtidal estuary, Dyfi River Estuary, west Wales, U.K. *Sed. Geol.*, **73,** 43–58.

Sieverding, J.L. and **Harris, P.M.** (1991) Mixed carbonates and siliciclastics in a Mississippian paleokarst setting, southwestern Wyoming thrust belt. In: *Mixed Carbonate-Siliciclastic Sequences* (Eds A.J. Lomando and P.M. Harris), *Proc. Soc. Sed. Geol. Core Workshop*, **15,** 541–568.

Southard, J.B., Young, R.A. and **Hollister, C.D.** (1971) Experimental erosion of calcareous ooze. *J. Geophys. Res.*, **76,** 5903–5909.

Storms, J.E.A., Weltje, G.J., Terra, G.J., Cattaneo, A. and **Trincardi, F.** (2008) Coastal dynamics under conditions of rapid sea-level rise: Late Pleistocene to Early Holocene evolution of barrier-lagoon systems on the northern Adriatic shelf (Italy). *Quat. Sci. Rev.*, **27,** 1107–1123.

Stride, A.H. (1982) *Offshore Tidal Sands: Processes and Deposits*. Chapman and Hall, New York, 222 pp.

Stupples, P. (2002) Tidal cycles preserved in late Holocene tidal rhythmites, the Wainway Channel, Romney Marsh, southeast England. *Mar. Geol.*, **182,** 231–246.

Sztanó, O. and **de Boer, P.** (1995) Basin dimensions and morphology as controls on amplification of tidal motions (the Early Miocene, North Hungarian Bay). *Sedimentology*, **42,** 665–682.

Tansi, C., Muto, F., Critelli, S. and **Iovine, G.** (2007) Neogene-Quaternary strike-slip tectonics in the central Calabrian Arc (southern Italy). *J. Geodyn.*, **43,** 393–414.

Tessier, B. (1998) Tidal cycles, annual versus semi-lunar records. In: *Tidalites: Processes and Products* (Eds C.R. Alexander, R.A. Davis and V.J. Henry), *SEPM Spec. Publ.*, **61,** 69–74.

Tessier, B. and **Gigot, P.** (1998) A vertical record of different tidal cyclicities: an example from the Miocene Marine Molasse of Digne (Haute Provence, France). *Sedimentology*, **36,** 767–776.

Thrana, C. and **Talbot, M.R.** (2006) High-frequency carbonate-siliciclastic cycles in the Miocene of the Lorca Basin (western Mediterranean, SE Spain). *Geol. Acta*, **4,** 343–354.

Tomkins, M.R., Nielsen, P. and **Hughes, M.G.** (2003) Selective entrainment of sediment graded by size and density under waves. *J. Sed. Res.*, **73,** 906–911.

Tortorici, L. (1982) Lineamenti geologico-strutturali dell'Arco Calabro Peloritano. *Soc. Ital. Mineral. Petrogr.*, **38,** 927–940.

Tortorici, L., Monaco, C., Tansi, C. and **Cocina, O.** (1995) Recent and active tectonics in the Calabrian Arc (southern Italy). *Tectonophysics*, **243,** 37–55.

Tropeano, M., Sabato, L., Cilumbriello, A., Gallicchio, S., Longhitano, S.G. and **Pieri, P.** (2006) *Sequence Stratigraphy – Advanced Course Field Manual*. Basilicata University, Potenza, 47 pp.

Turco, E., Maresca, R. and **Cappadona, P.** (1990) La tettonica plio-pleistocenica del confine calabro-lucano: modello cinematico (Plio-Pleistocene tectonics at the Calabrian-Lucanian boundary: a kinematic model). *Mem. Soc. Geol. Ital.*, **45,** 519–529.

Vai, G.B. (2001) Structure and stratigraphy: an overview. In: *Anatomy of an Orogen: The Apennines and Adjacent Mediterranean Basins* (Eds G.B. Vai and P.I. Martini), pp. 15–32. Kluwer Academic Publishers, Dordrecht.

Van Dijk, J.P., Bello, M., Brancaleoni, G.P., Cantarella, G., Costa, V., Frixa, A., Golfetto, F., Merlini, S., Riva, M., Torricelli, S., Toscano, C. and **Zerilli, A.** (2000) A regional structural model for the northern sector of the Calabrian Arc (southern Italy). *Tectonophysics*, **324,** 267–320.

Vercelli, F. (1925) *Il regime delle correnti e delle maree nello Stretto di Messina. Commissione del Mediterraneo, Venezia.* Campagnes du Marsigli Report, Venice, 22 pp.

Visser, M.J. (1980) Neap-spring cycles reflected in Holocene subtidal large-scale bedform deposits: a preliminary note. *Geology*, **8,** 543–546.

Walker, R.G. and **Plint, A.G.** (1992) Wave- and storm-dominated shallow marine systems. In: *Facies Models – Response to Sea Level Changes* (Eds R.G. Walker and N.P. James), pp. 219–238. Geological Association of Canada, St John's.

Warzeski, R.E., Cummingham, K.J., Ginsburg, R.N., Anderson, J.B. and **Zan-Dong, D.** (1996) A Neogene mixed siliciclastic and carbonate foundation for the Quaternary carbonate shelf, Florida Keys. *J. Sed. Res.*, **66,** 788–800.

Wells, M.R., Allison, P.A., Hampson, G.J., Poggott, M.D. and **Pain, C.C.** (2005) Modelling ancient tides: the Upper Carboniferous epi-continental seaway of Northwest Europe. *Sedimentology*, **52,** 715–735.

Williams, G.E. (1991) Upper Proterozoic tidal rhythmites, South Australia: sedimentary features, deposition, and implications for the earth's palaeorotation. In: *Clastic Tidal Sedimentology* (Eds D.G. Smith, G.E. Reinson, B.A. Zaitlin and R.A. Rahmani), *Can. Soc. Petrol. Geol. Mem.*, **16,** 161–177.

Wright, E.E., Hine, A.C., Goodbred Jr, S.L. and **Locker, S.D.** (2005) The effect of sea-level and climate change on the development of a mixed siliciclastic-carbonate, deltaic coastline: Suwannee River, Florida, U.S.A. *J. Sed. Res.*, **75,** 621–635.

Yang, C.S. and **Nio, S.D.** (1985) The estimation of paleohydrodynamic processes from subtidal deposits using time series analysis methods. *Sedimentology*, **32,** 41–57.

Yose, L.A. and **Heller, P.L.** (1989) Sea-level control of mixed-carbonate-siliciclastic, gravity-flow deposition: lower part of the Keeler Canyon Formation (Pennsylvanian), southeastern California. *Geol. Soc. Am. Bull.*, **3,** 427–439.

Young, R.A. and **Mann, R.** (1985) Erosion velocities of skeletal carbonate sands, St. Thomas, Virgin Islands. *Mar. Geol.*, **69,** 171–185.

Young, R.A. and **Southard, J.B.** (1978) Erosion of fine grained marine sediments: sea-floor and laboratory experiments. *Geol. Soc. Am. Bull.*, **89,** 663–672.

Zecchin, M., Massari, F., Mellere, D. and **Prosser, G.** (2004) Anatomy and evolution of a Mediterranean-type fault bounded basin: the Lower Pliocene of the northern Crotone Basin (Southern Italy). *Basin Res.*, **16,** 117–143.

Zuffa, G.G. (1980) Optical analyses of arenites: influence of methodology on compositional results. In: *Provenunce of Arenites* (Ed. G.G. Zuffa), pp. 165–189. Reidel Publishing Company, Dordrecht.

Zuffa, G.G. (1985) Hybrid arenites: their composition and classification. *J. Sed. Petrol.*, **50,** 21–29.

Manuscript received 29 September 2009; revision accepted 25 May 2010